USCIPI Report 900

ANNUAL TECHNICAL REPORT

April 15, 1978 - April 14, 1979

# NONLINEAR REAL-TIME OPTICAL SIGNAL PROCESSING

A.A. Sawchuk, Principal Investigator
T.C. Strand, A.R. Tanguay, Jr., A. Armand,
J. Michaelson, and M. Muha

June 15, 1979

Department of Electrical Engineering
Image Processing Institute
University of Southern California
Los Angeles, California 90007

Research sponsored by the
Air Force Office of Scientific Research
Electronics and Solid State Sciences Division
under Grant No. AFOSR-77-3285

UNCLASSIFIED

SECURITY CLASSIFICATION OF THIS PAGE (When Data Entered)

| REPORT DOCUMENTATION PAGE | | READ INSTRUCTIONS BEFORE COMPLETING FORM |
|---|---|---|
| 1. REPORT NUMBER<br>USCIPI Report 900 | 2. GOVT ACCESSION NO. | 3. RECIPIENT'S CATALOG NUMBER |
| 4. TITLE (and Subtitle)<br>Nonlinear Real-Time Optical Signal Processing | | 5. TYPE OF REPORT & PERIOD COVERED<br>Annual Report<br>4/15/78 to 4/14/79 |
| | | 6. PERFORMING ORG. REPORT NUMBER<br>USCIPI Report 900 |
| 7. AUTHOR(s)<br>A.A. Sawchuk, T.C. Strand, A.R. Tanguay, Jr.,<br>A. Armand, J. Michaelson, M. Muha | | 8. CONTRACT OR GRANT NUMBER(s)<br>AFOSR-77-3285 |
| 9. PERFORMING ORGANIZATION NAME AND ADDRESS<br>Department of Electrical Engineering<br>Image Processing Institute<br>University of Southern California<br>Los Angeles, Calif. 90007 | | 10. PROGRAM ELEMENT, PROJECT, TASK AREA & WORK UNIT NUMBERS |
| 11. CONTROLLING OFFICE NAME AND ADDRESS<br>Air Force Office of Scientific Research<br>Bldg. 410, Bolling AFB<br>Washington, D.C. 20332 | | 12. REPORT DATE<br>June 15, 1979<br>13. NUMBER OF PAGES<br>72 |
| 14. MONITORING AGENCY NAME & ADDRESS(if different from Controlling Office)<br>As above | | 15. SECURITY CLASS. (of this report)<br>Unclassified<br>15a. DECLASSIFICATION/DOWNGRADING SCHEDULE |

16. DISTRIBUTION STATEMENT (of this Report)

The United States Government is authorized to reproduce and distribute reprints for Governmental purposes notwithstanding any copyright notation hereon.

17. DISTRIBUTION STATEMENT (of the abstract entered in Block 20, if different from Report)

18. SUPPLEMENTARY NOTES

19. KEY WORDS (Continue on reverse side if necessary and identify by block number)

Optical information processing
Nonlinear optical processing
Real-time optical processing
Optical computing

20. ABSTRACT (Continue on reverse side if necessary and identify by block number)

The results of the second year of a two year research program in nonlinear real-time optical signal processing are described. The goal of the program is to extend fast parallel nonlinear operations to optical processing systems with large time-bandwidth and space-bandwidth products. Several approaches have been investigated. The most mature technique involves the parallel filtering of a pulse-width modulated continuous input obtained by

DD FORM 1 JAN 73 1473 EDITION OF 1 NOV 65 IS OBSOLETE

UNCLASSIFIED

SECURITY CLASSIFICATION OF THIS PAGE (When Data Entered)

TABLE OF CONTENTS

## ABSTRACT

The results of the second year of a two year research program in nonlinear real-time optical signal processing are described. The goal of the program is to extend fast parallel nonlinear operations to optical processing systems with large time-bandwidth and space-bandwidth products. Several approaches have been investigated. The most mature technique involves the parallel filtering of a pulse-width modulated continuous input obtained by halftoning and hard-clipping with real-time optical input devices. Real-time homomorphic and logarithmic filtering has been achieved by this method. A complete analysis of the system degradations due to non-ideal real-time devices has been made and several methods to compensate for these effects are described and experimentally verified. A second technique uses the inherent nonlinear characteristics of a real-time device to achieve nonlinear functions in incoherent illumination without halftoning. An experimental three bit parallel optical analog-to-digital converter based on this principle is described. Another technique uses multiple liquid crystal light valves (LCLV's) to achieve electronically programmable time variable optical nonlinearities. A last technique uses the variable grating mode (VGM) of LCLV's to perform local frequency modulation as a function of the image brightness for nonlinear processing by selection and recombination of these frequencies. An experimental VGM LCLV and level slicing results are described. The project has been a joint effort between the University of Southern California Image Processing Institute (USCIPI) and the Hughes Research

Laboratories (HRL), Malibu, California. The USC group has developed new systems and techniques for nonlinear optical processing and the HRL group has performed work on various real-time devices.

# 1. RESEARCH PROGRESS

## 1.1 Introduction and Project Overview

This report summarizes the results of the second year of a two year research effort in performing nonlinear operations in optical signal processing and achieving operation in real time using various input transducers. Section 1.1 contains an introduction, motivation for the work and an overview of the research program. Detailed descriptions of specific results are contained in later sections.

### 1.1.1 Introduction and Motivation

There is a great general need for systems which can perform fast, parallel multi-dimensional operations on signals with large time-bandwidth and space-bandwidth products. These needs arise in terminal guidance, nonlinear tracking and signal filtering, imaging radar systems, image processing, image target and pattern recognition and automated assembly [1,2]. In many of these applications, electronic analog and digital hardware is inadequate.

The parallel nature of optical systems and their inherently large space-bandwidth product has led to the development of many systems and techniques for optical information processing. A fundamental difficulty with optical processing has been the limited range of operational "software" available [3]. Thus, general nonlinear operations such as logarithms, power law, and limiters have been very hard to implement. The usual types of coherent and incoherent optical processors are essentially limited to the linear operations of

correlation, convolution, and filtering [4]. Many new techniques of signal processing and pattern recognition require nonlinear functions as part of their operation, and these functions have been achieved digitally, although in serial form [2,4]. Certain particular optical nonlinearities have been achieved in the past using special techniques, but these methods are clumsy, hard to repeat and control, and often are limited in dynamic range.

A second major difficulty of optical information processing is the problem of input and output [5]. Recent developments have simplified the output problem: television and solid-state devices are available to efficiently make use of the two-dimensional processed output. In many situations, the human eye or observer is the end user of the information, so that optical systems with their inherent two-dimensional nature are ideally suited to process pictorial information intended eventually for the human observer. The major difficulty lies with real-time input to optical processors. Flexible real-time optical input modulators which can convert electronic or image information into a form for input to a processing system are badly needed, and significant research over the last several years has made progress on certain aspects of this problem. Thus, combined work on these two major limitations to optical information processing is the subject of this research.

### 1.1.2 Project Overview

This program has been a joint cooperative effort between the University of Southern California (USC) group and the Hughes Research

Laboratories (HRL) in Malibu, California. Each group has participated together in the project since its beginning in April 1977 and a separate progress report is being submitted by HRL as a companion to this report. The expertise of the USC group lies in the creation of new techniques for nonlinear processing and in the development of real-time electro-optical input devices for optical processing. Members of the USC group have been involved in nonlinear optical processing work for several years. The expertise of the HRL group is in the development and extension of liquid crystal light valve (LCLV) technology for real-time implementation of new and existing techniques of nonlinear optical signal processing. The HRL group is one of the leaders in LCLV technology and have developed an advanced, commercially available transducer for linear real-time processing [25,26].

Halftone Processing

Because of the recent emergence of the two technologies of nonlinear processing and real-time input transducers, no particular combination of methods has appeared clearly superior and many alternatives were explored during the first year of work in this project. A major part of the first and second year's effort has been concerned with real-time halftone nonlinear processing. This method involves the conversion of a two-dimensional input signal with continuous levels to a pulse-width modulated binary input for use with an optical filtering system. Prior to a real-time implementation of haltone processing, many nonlinear functions such as logarithms [6,9],

exponentiation [9], level slicing [8,9], multiple isophote generation [7,12], quantization [10], pseudocolor [13], and A-D conversion [7,14] were implemented.

More recently, attention has been given to different aspects of halftone nonlinear processing. The important aspects include halftone screen synthesis algorithms [8-11], halftone screen fabrication techniques [9,10], and halftone recording and processing techniques [7]. Synthesis algorithms that generate the halftone screen profiles for the periodic cells of ordinary monotonic screens [8], or cell profiles which are nonmonotonic [10] have been developed.

The ideal real-time device for halftone nonlinear processing has a perfect hard-clipping binary characteristic curve and large saturation density. Problems with the use of non-ideal devices had been investigated in earlier studies, and during this second year of work an accurate general analysis which considers these characteristics has been completed [15,18,20]. From this analysis, the output degradation due to the recording medium characteristic curve can be found for any desired nonlinear transformation [20].

The problem of designing the halftone screen cell shape has been analyzed for a piecewise linear recording medium. The problem reduces to the solution of a nonlinear integral equation which can be solved for a certain types of monotonic nonlinear functions, including exponential and power law transformations. For the general solution, an approximate method which considers a discrete halftone screen density profile has been developed. This gives the halftone screen

density profile for any form of recording medium characteristic and any type of nonlinearity. The method minimizes the mean-square difference between the desired and degraded outputs.

A summary of this second year of work on real-time halftone processing is given in sections 1.2 and 1.3 of this report. Section 1.2 describes the theory for degradations due to the soft threshold of the real-time device and outlines techniques for precompensation. Section 1.3 shows recent experimental results in real-time logarithmic and homomorphic filtering. Many additional details on halftone processing are contained in the USCIPI Report 880 "Real-Time Nonlinear Optical Information Processing" by A. Armand [20], which is being distributed as a companion to this yearly progress report. Rather than repeating these results here, the interested reader can refer to this publication.

Significant future progress on real-time nonlinear halftone processing still awaits the development of a high contrast high resolution real-time device. Although many possible candidate ideas have emerged from this study, no immediately available breakthroughs which will lead to such a device have been found. Other Hughes work on silicon photoconductor light valves shows promise of high contrast operation, but the problem of extreme resolution needed because of the gray scale-pulse width modulation tradeoff in halftoning still is a major limitation. The HRL annual progress report on Contract No. F4620-77-C-0080 is a companion to this report and describes details of the light valve development. Another disadvantage is that

coherent light is needed for nonmonotonic functions, and this carries with it problems of speckle, phase uniformity and the need for a laser source. It is expected that future work in nonlinear processing will concentrate on methods other than halftoning.

Direct Nonlinear Processing

An alternate technique for nonlinear optical processing directly uses the inherent nonlinear characteristics of a real-time device to achieve nonlinear functions without halftone preprocessing [15-17,19]. The general technique involves the selection of operating points on a nonlinear device curve to directly achieve a point-by-point mapping. The method shows promise because it could operate with incoherent illumination, avoiding speckle, phase noise and laser sources. No halftone screen is needed, so that device resolution requirements would be much lower. A drawback is that the flexibility of the technique is limited to certain types of functions. Detailed progress and experimental implementation are described in Section 1.4.

Multiple Light Valve System

During the past year an experimental system using several different types of LCLV's has been assembled to do general nonlinear processing. The system can be electronically programmed to change the available nonlinear function with time. An experimental implementation is described in Section 1.5. Work on this project will continue in the future, and, as with other real-time nonlinear processing methods, its ultimate accuracy and flexibility depend on

the quality of available LCLV's. These issues are discussed in detail in Section 1.5.

Variable Grating Mode Processing

Another method of nonlinear optical processing currently under study involves the conversion of different input levels to a local phase-modulated input whose spatial frequency is a function of the brightness. The conversion takes place in a special real-time LCLV device which forms a spatial grating structure as a function of voltage or applied illumination. This technique is called variable grating mode (VGM) processing [15-17,19]. When the variable grating is placed in the front focal plane of a coherent Fourier transform processor, the difference in local spatial frequency causes different input levels to be effectively placed at different points in the transform plane. By selective filtering and recombination of the transform components, various nonlinearities can be achieved. A theoretical analysis of this method and preliminary experimental results are given in Section 1.6.

Alternative Devices for Nonlinear Optical Processing

In parallel to the HRL effort in developing real-time LCLV devices, we have explored several new alternative technologies for real-time devices suitable for nonlinear processing. The results of this work are given in Section 1.7. The areas of study are: a) devices with sharp threshold characteristics; b) Pockels Readout Optical Modulator (PROM) type devices; and c) devices utilizing

sputtered thin films.

## 1.2 Halftone Processing: Theory of Soft Threshold Effects and Precompensation

To realize nonlinear halftone processing in real-time, the high-contrast photographic recording medium used in this process should be replaced with a real-time image transducer. To obtain ideal results, such a transducer should have a sharp threshold characteristic. The presently developed real-time image converters, like the standard liquid crystal light valve (LCLV), do not possess this characteristic. To predict the effects of the nonideal characteristic of the LCLV on the halftone process a general formulation was developed. The details of this formulation can be found in a companion to this report, USCIPI Report 880 [20]. This formulation relates the output of the nonlinear process to the input through the halftone screen parameters and through the real-time device characteristic curve. To find out how different parts of the characteristic curve of the real-time device affect the output of the process, we have used the hafltone screen density profile that is designed for the binary recording medium and some model characteristic curves which are binary in every respect except for a certain region. By simulating the entire nonlinear process with each of these screens, their performance can be compared directly. The results show that for smooth monotonic functions, e.g. logarithm, the main source of degradation of the output is the linear section of the characteristic curve as shown in Fig. 1.2-1. The shoulder and toe regions have less affect on the performance. For nonlinearities with sharp slope changes and sharp corners, such as the level slice function, the sharp

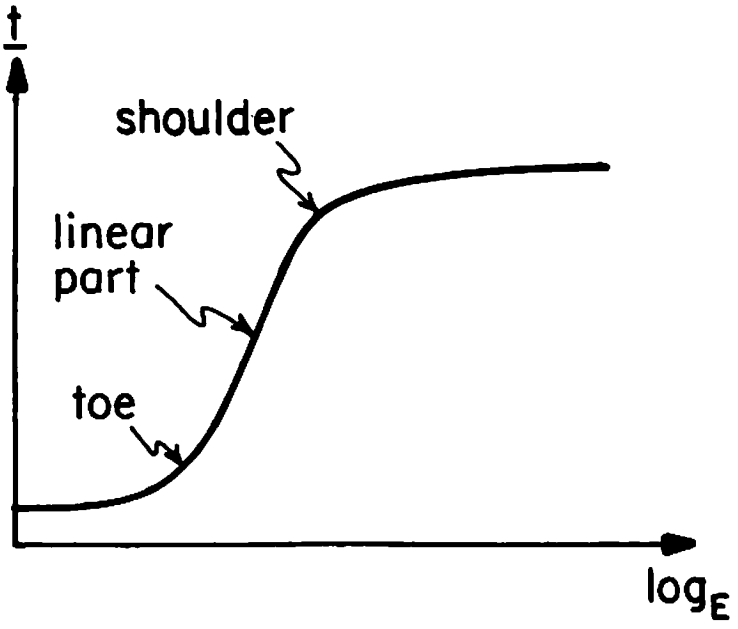


Figure 1.2-1 Typical characteristic curve of a nonbinary recording medium.

rises and falls become linear rather than abrupt and the sharp corners become rounded.

We have found two procedures to compensate for the nonbinary characteristic of the real-time device. In one method, the halftone screen cell shape is determined by inverting an integral equation. Although this method is exact, it is restricted to certain monotonic nonlinearities like power and exponential transformations and is restricted to a piecewise linear model for the recording medium characteristic curve. In the second method, the halftone screen density profile is quantized. The quantized density values are determined by minimizing in the mean-square sense the difference between desired and degraded outputs. This method can be used for any form of the recording medium characteristic curve and any type of nonlinearity. The result of a computer simulation for a logarithmic function is shown in Fig. 1.2-2. For this simulation it was assumed that there were 30 discrete points in the halftone screen density profile and that the screen density values were between 0 and 2. Note that the plot is semi-logarithmic and hence the ideal result is a straight line. The optimized output curve is seen to approximate the ideal result with a small error.

The same result for a level slice function is shown in Fig. 1.2-3. It is seen that the optimization procedure is successful in improving the fit to the level slice function, but cannot do much for the edges with finite slope in the degraded response.

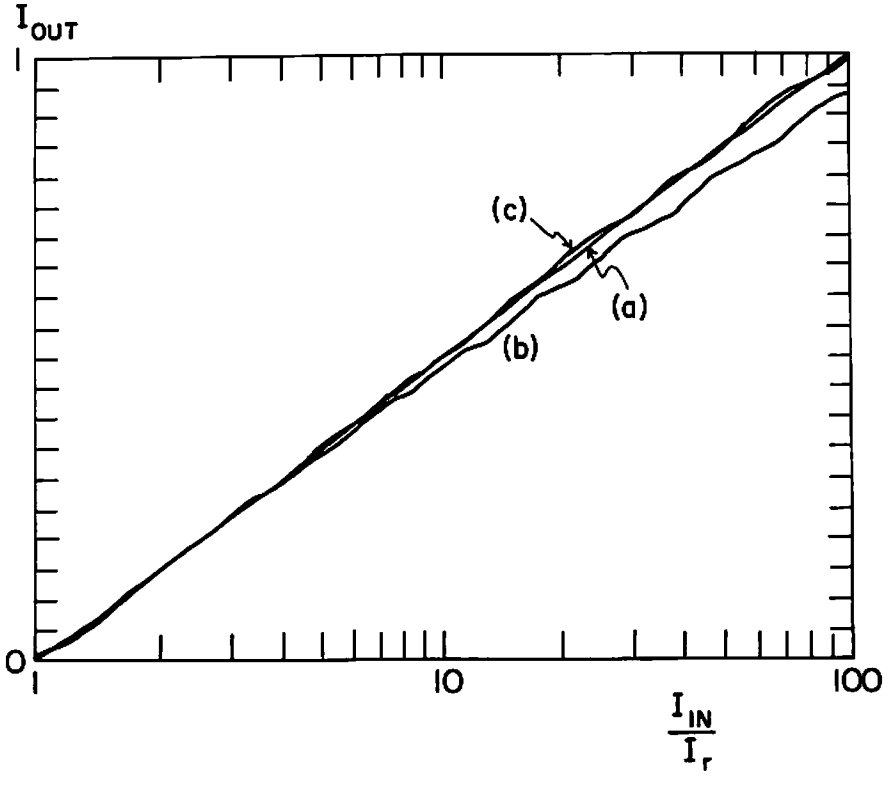


Figure 1.2-2 Logarithmic characteristics.

a) Ideal response
b) Degraded response for a medium with a gamma of 3.
c) Optimized response for a medium with a gamma of 3.

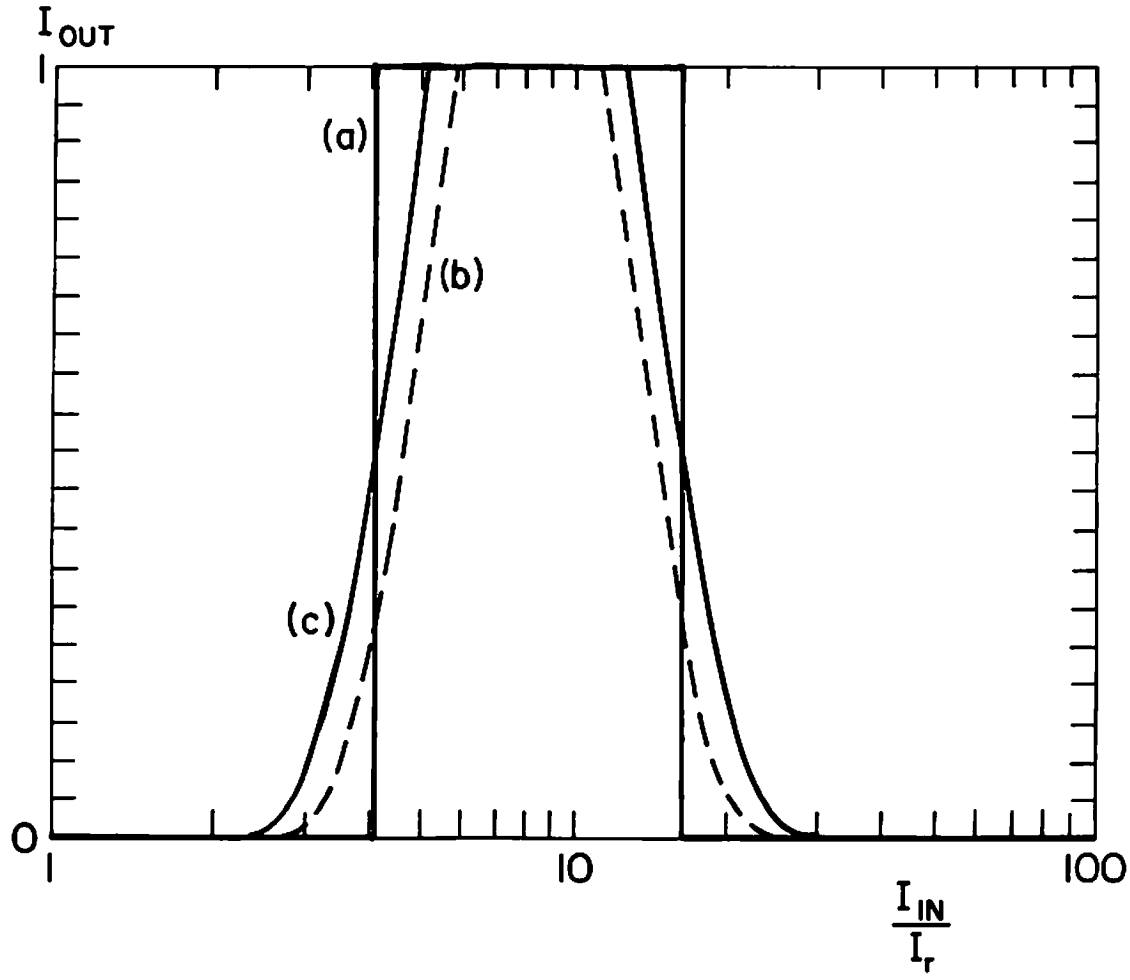


Figure 1.2-3 Level slice characteristics.

a) Ideal response
b) Degraded response for a medium with a gamma of 3.
c) Optimized response for a medium with a gamma of 3.

## 1.3 Halftone Processing: Experimental Results

To demonstrate real time halftone processing, a halftone screen was fabricated to produce a logarithmic characteristic curve in conjunction with a particular LCLV. This nonlinearity was chosen because of its utility in such applications as homomorphic filtering [21].

Figure 1.3-1 shows the measured response curve of a LCLV along with the response curve of the halftone processing system with the halftone screen in place. With the halftone screen a reasonably logarithmic response is obtained over the design range of two decades.

The next step was to apply this system to an image filtering experiment. For this experiment a picture with multiplicative noise was generated. The goal was to eliminate the multiplicative noise by homomorphic filtering; i.e., a sequence of a logarithmic transformation followed by linear filtering. Ideally, this would be followed by an exponential transformation but this is not essential in demonstrating noise reduction [6]. The exponentiation was not included in the following experiments. The noise generated for this experiment models that of a push-broom scanner that scans six lines at a time with six independent detectors. Any variation in the sensitivity or gain along the row of detectors gives rise to a periodic six-bar noise structure across the image. This effect is shown in Fig. 1.3-2a. The density range of the image with the simulated scanner noise was 2.0D. This was chosen to match the 100:1 operating range of the halftone screen.

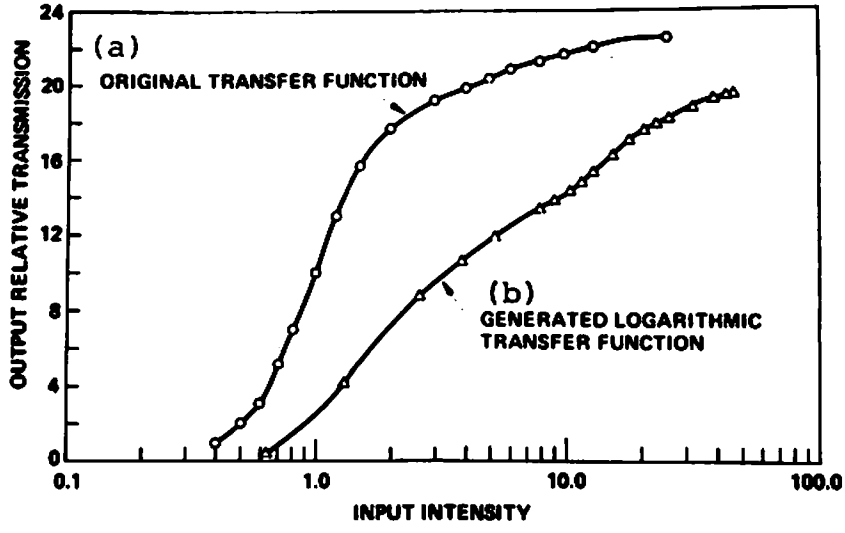


Figure 1.3-1 Liquid crystal light valve transfer function.
a) Without Halftone Screen.
b) With Halftone Screen.

a) Original object with multiplicative scanner noise.

b) Image after homomorphic filtering.

Figure 1.3-2 Real-time homomorphic filtering.

The noisy image was sandwiched with the halftone screen and imaged with incoherent illumination onto the LCLV. The resultant image was read out with a HeNe laser. A spatial filter was placed in the Fourier plane of the system to select a single (zeroth) diffraction order in the halftone spectrum. Since the screen effectively performs a logarithmic transformation, the pattern in the zeroth diffraction order of the Fourier plane consisted of the sum of the image diffraction pattern and the pushbroom scanner diffraction pattern. The scanner diffraction pattern consisted of a series of isolated diffraction orders which could be filtered out without significantly degrading the image. Thus in the output plane the image is reconstructed without the multiplicative noise. This is shown in Fig. 1.3-2b. Without the logarithmic transformation, the noise and image spectra would have been convolved with one another making them impossible to separate.

This experiment demonstrates the feasibility of performing real-time nonlinear filtering using compensated halftne screens in conjunction with the LCLV or other real-time device. In particular this experiment demonstrates the feasibility of performing homomorphic filtering in real time.

## 1.4 Direct Nonlinear Processing

An important part of this year's work was the direct optical nonlinear function achieved without the use of halftone screens or variable phase gratings. This method relies directly on the nonlinear nature of electro-optical devices such as the LCLV or Pockels Readout Optical modulator (PROM) device [22-24]. Both these two devices and many other real-time optical input transducers rely on electrooptically controlled birefringence to produce a selective linear differential phase retardation along two axes of a crystal. When the crystal is placed between crossed polarizers, a sinusoidal variation of intensity transmittance with voltage is produced as shown in Fig. 1.4-1. This nonlinear nonmonotonic behavior is the basis for many possible optically controlled nonlinear functions. By placing a photoconductor near the crystal surface, (as in the LCLV) the local voltage is variable in a two-dimensional manner by applying a control image. In the PROM device, the crystal itself is a photoconductor at certain control wavelengths. The particularly interesting fact is that the system can be controlled and operated in strictly incoherent light. No diffraction or Fourier transforming is needed. Also, the spatial frequency resolution requirements are much lower because sharp edges of binary dots as in halftoning do not have to be maintained.

A particularly useful function is the optical parallel A/D converter. Here an array of parallel electron thresholding devices in the output plane of the system is needed to sense the separate bit planes of a binary output. If thresholds were set at 1/2 in the three

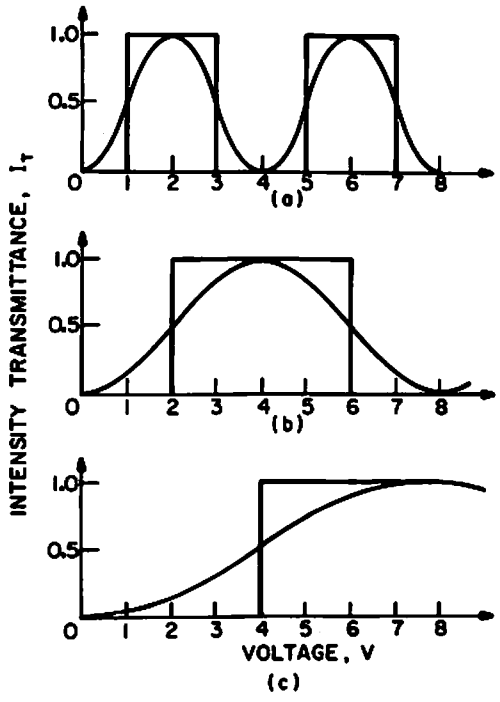


Figure 1.4-1 Analog-to-digital converter bit planes for three bit Gray code.

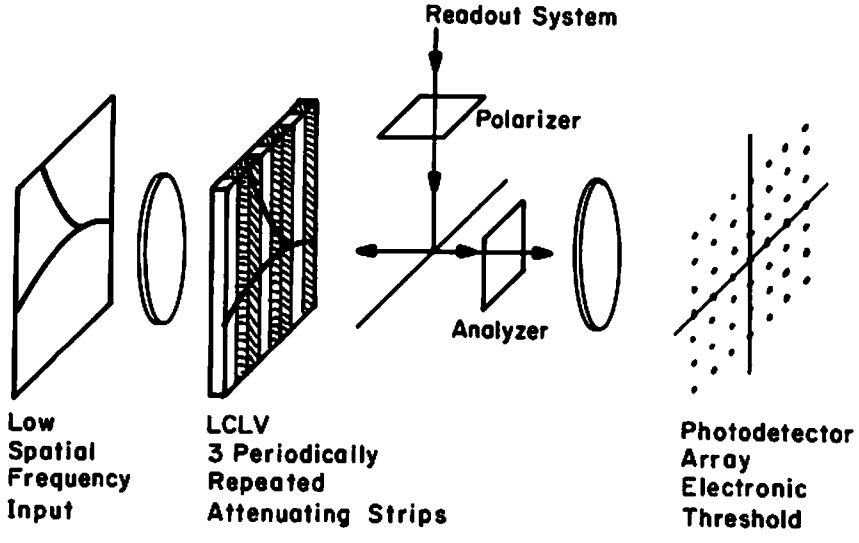


Figure 1.4-2 System for parallel A/D conversion.

device curves of Fig. 1.4-1, then a 1 output would be produced above threshold and a zero output below as shown by the square jump functions plotted. This electronic thresholding is easily done by a parallel array of light detectors and sensors, and is an essential part of the system replacing the optical thresholding as in halftoning. The three curves of Fig. 1.4-1 represent the 3 bits of an optical A/D converter whose output is in the reflected binary or gray code. Note that any continuous input between 0 and 8 gives a unique 3 bit code. The system could operate in parallel with an interfaced array of detectors matched to selected photoconductor strips with the required voltage characteristics. The system could also operate serially using the characteristics of Fig. 1.4-1a. Using the full dynamic range (0 to 8) gives the least significant bit. The input light is then attenuated by a factor of one-half (to the range 0 to4) so that the effective response is the same as Fig. 1.4-1b. The final (most significant) bit is obtained by using an attenuation of 4 so the curve of Fig. 1.4-1c is the effective result. Other A/D code coversions such as the usual straight binary code can be achieved by translating these curves left or right along the V axis. This can be done by introducing phase retardation plates with different delays along orthogonal axes into the crossed polarizer system.

In the past year the first real-time A/D conversion using the direct nonlinear characteristic of an optical device was achieved [16,17,19]. Three bit planes were generated using a liquid crystal device supplied by HRL. The device was a perpendicularly aligned nematic liquid crystal with a CdS photoconductor.

The experimental setup is essentially as shown in Fig. 1.4-2. In the actual setup there were no attenuating strips on the LCLV. This meant that the bit planes had to be generated serially. Also, the output was recorded on hardclipping film rather than a thresholding detector array. The input object illumination is strictly incoherent. The output, or read beam is derived from an arc lamp passed through an interference filter. A narrow spectral bandwidth is required on readout due to the dispersion of the birefiringence.

As the input illumination intensity is increased, the output intensity varies in a quasi-sinusoidal fashion due to the changing birefringence. If the amount of birefringence varied linearly as a function of a write beam intensity, one would expect a strictly sinusoidal variation of the output intensity. However a number of factors, including the optical nature of the liquid crystal and the photoconductor and the electrical properties of the liquid crystal, affect the output characteristic and produce an approximately sinusoidal output whose frequency varies (monotonically) with input intensity. Figure 1.4-3 is the measured response curve of one of the devices.

Although the theory behind the A/D conversions assumes a strictly periodic response characteristic, it is in general possible to produce the desired bit planes using the quasi-periodic response curves of actual devices. The trade-off that must be made is that one must resort to a non-uniform quantization. The quantization levels used in the A/D experiment are indicated Fig. 1.4-3.

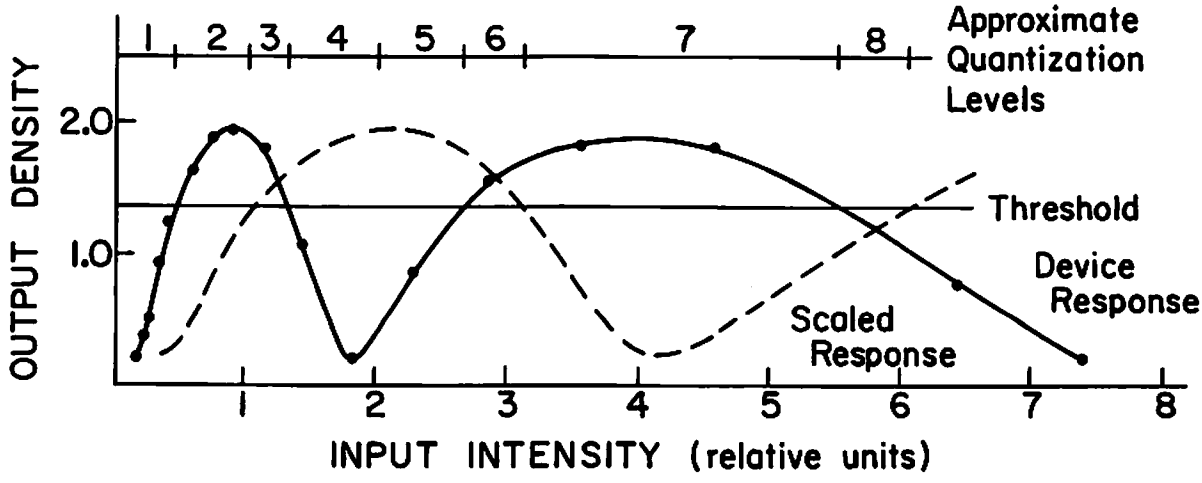


Figure 1.4-3 Response curve of the LCLV used for the three bit A/D conversion. The solid curve is the measured response. Hardclipping this curve at the indicated threshold produced the least significant bit-plane. The dotted curve represents the same response with a fixed attenuation of the input intensity. Hard-clipping this produced the second bit-plane. The eight quantization levels of the resulting three bit code are indicated at the top.

To test the A/D concept a test target was generated consisting of an eight gray level step tablet. The gray levels were chosen to match the quantization levels shown in Fig. 1.4-3. This test object was imaged on to the LCLV and the output was photographically hardclipped. This produced the least sigficant bit-plane of a three-bit A/D conversion. Next the write illumination intensity was decreased, effectively rescaling the device response curve to generate the next bit-plane. The last bit-plane (most significant bit) was obtained by attenuating the write intensity again and photographing the output. The input and the three bit-planes thus generated are shown in Fig. 1.4-4. The bit plane images suffer from noise, however most of this noise can be traced back to the original test target which was produced using the DICOMED image recorder and Kodak SO-115 film. It is felt that these results could be considerably improved by reducing the noise in the original.

These results represent the first real-time parallel A/D conversion to be performed on two-dimensional input. The A/D conversion bit rate potential can be estimated from typical parameters of devices currently available. The important parameters are device resolution which is typically 40 line pairs/mm, device size which is on the order of 50mm by 50mm, and speed which is generally designed for 30 frames/second. Multiplying all the parameters together implies an A/D conversion rate of $1.2 \times 10^8$ points processed per second. The fast parallel nature of the device makes it suitable for digitizing images or other page organized data without the need for scanning.

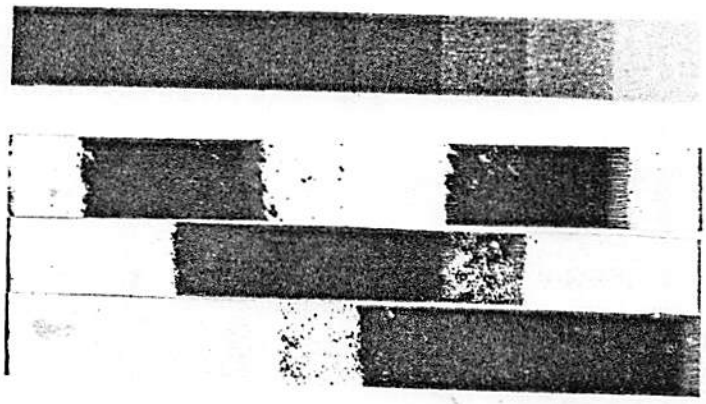

Fig. 1.4-4 Direct analog-to-digital conversion. The eight level analog input is shown at the top. Below is the binary coded output in the form of three bit-planes of the Gray code.

Although these initial results are quite encouraging, actual application of this technique must await improved recording devices. There are two particular device related problems which need to be addressed. First is the aperiodic nature of the overall device response. As was seen in the experimental work, this results in unequal quantization intervals and limits the number of bits which can be generated in the A/D conversion. Although the LCLV is inherently aperiodic due to the nonlinear response of the photoconductor and the nonlinear relationship between applied voltage and the effective birefringence, other devices promise a response with good periodicity. The second problem is one of uniformity of response over the face of the device. Although this is certainly a difficult problem, it is not an inherent problem and thus should prove solvable by improved production methods.

## 1.5 Multiple Light Valve System

During the last period of effort a new type of LCLV system containing several light valves has been evaluated. The system performs nonlinear processing in real-time and has the advantages of incoherent operation and electronic programming of arbitrary nonlinearities. The system has been assembled with experimental light valves obtained from Hughes Research Laboratories (HRL) and is called the multiple light valve system (MLVS).

A functional schematic of the MLVS is shown in Fig. 1.5-1. The first element in the system maps the intensity variations of the two-dimensional input image into two-dimensional outputs with constant magnitude and temporal separation. This step is done by a time-scanning level slice produced with a LCLV. The constant magnitude outputs are then weighted as a function of time by another LCLV to give the desired nonlineear transformation. The weighted outputs are then integrated over an appropriate time interval to give a nonlinearly transformed output image. The operation is shown schematically in Fig. 1.5-1 for a simple three intensity level, two dimensional input image. The intensity-to-time converter maps input intensities over the range of 0 to $I_{max}$ into the time interval [0,T]. Thus for a linear mapping, the output plane for the intensity-to-time converter will remain dark during the time interval $0<t<t_1$ since there are no intensity components in the input image between $I = 0$ and $I = I_1$. At time $t_1$ corresponding to the input intensity $I_1$, the output plane will have a constant intensity response over all portions

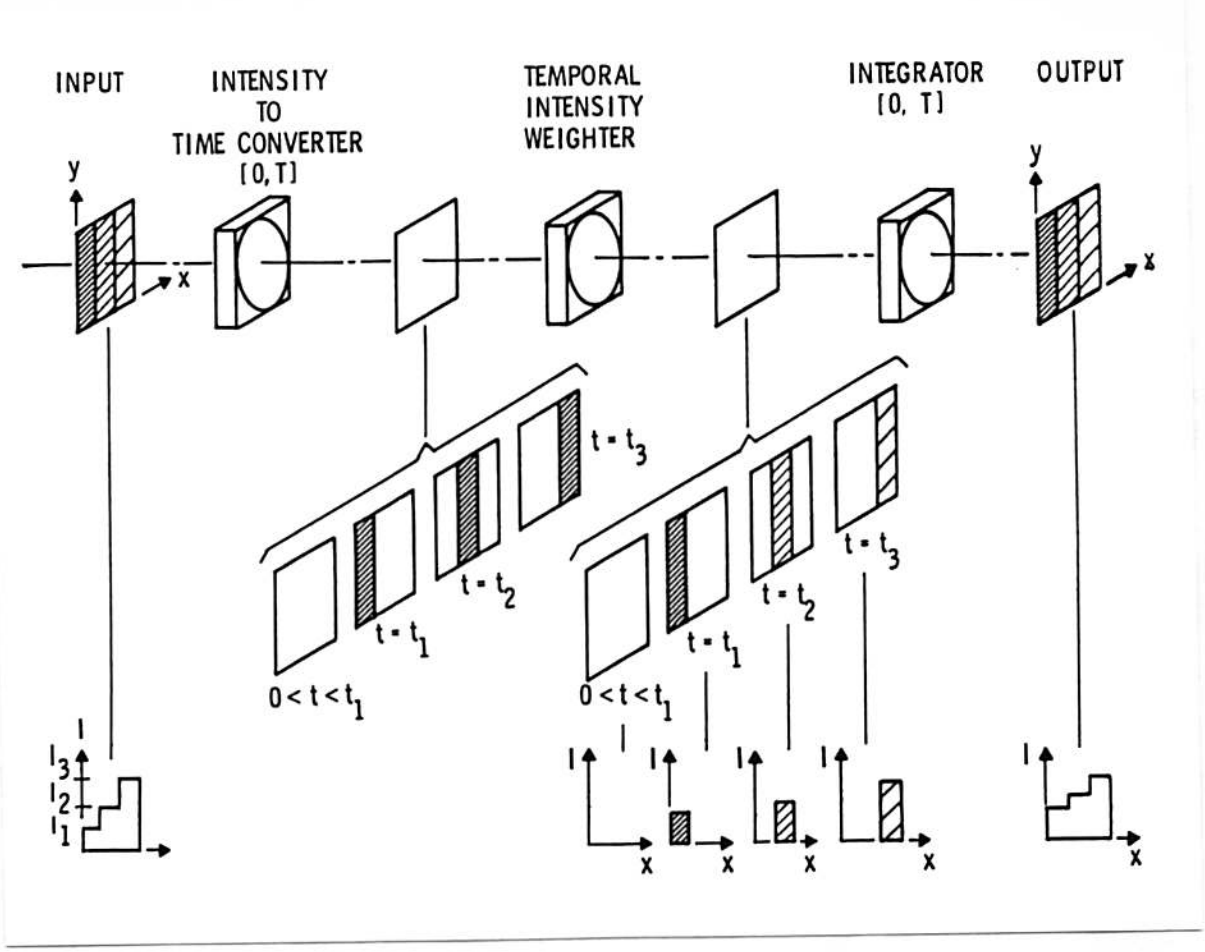


Figure 1.5-1 Functional schematic of the multiple light valve system (MLVS).

of the input image for which $I = I_1$. Similar output responses occur at times $t_2$ and $t_3$ as shown in the figure. For all other times $0<t<T$ with $t \neq t_1, t_2, t_3$ the output intensity remains at zero. The temporal intensity weighter is simply an electrooptic attenuator which weights the constant intensity, time sequential outputs of the intensity-to-time converter in the desired nonlinear manner. The time sequential weighted responses are then summed over the interval [0,T] in the integrator. Thus at time $t = T$, a nonlinearly transformed input image will be present at the integrator output. A simple logarithmic compression is depicted in Fig. 1.5-1.

One of the key features of the system is the ability to arbitrarily change the form of the nonlinear function in real time. The nonlinearity is introduced by applying a nonlinearly shaped voltage waveform into the temporal intensity weighter during the time interval [0,T]. In the system being evaluated, the waveform is produced by a microprocessor/D-A converter and can arbitrarily be changed to effect numerous trnsformations including logarithm, exponentiation, level slice, and A/D conversion.

Details of the implementation are shown in Fig. 1.5-2. In this figure, $LCLV_1$ performs the intensity-to-time conversion. The device is operated in a reflection mode and utilizes a CdS/CdTe heterojunction photoconductor. Two different devices have been used to implement this function, one with parallel liquid crystal surface alignment and the other with perpendicular alignment. In both cases alignment was uniform through the LC layer in the zero field state.

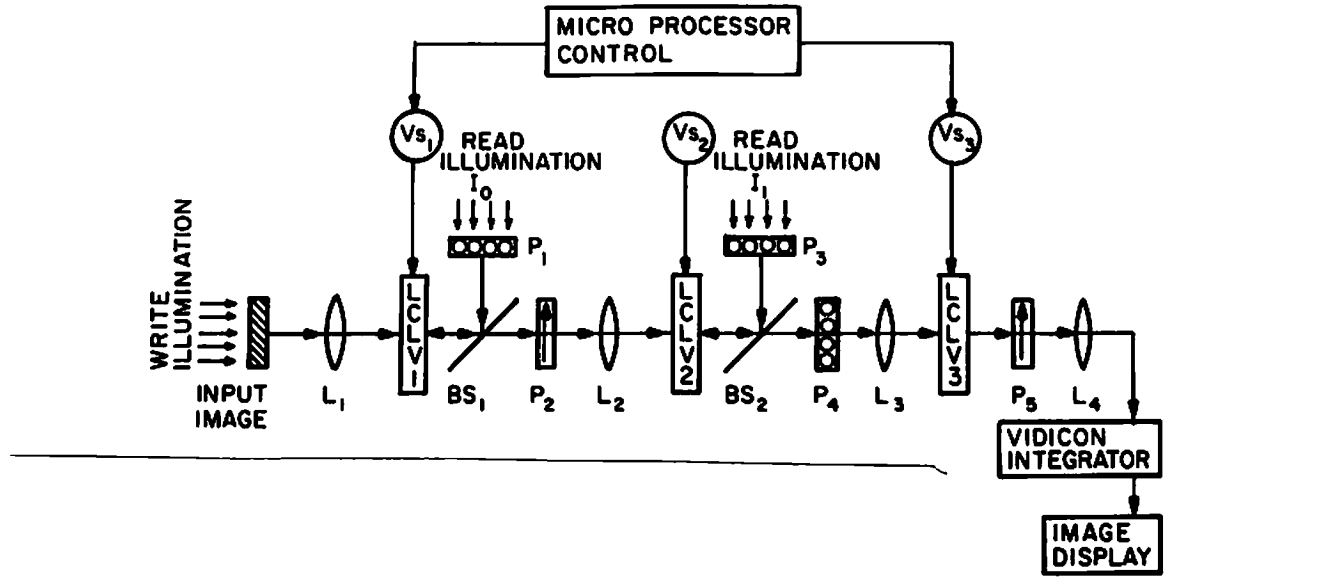


Figure 1.5-2 Block diagram of the multiple light valve system (MLVS).

Both devices gave similar system results.

For the case of parallel alignment, the phase retardation versus voltage characteristics of the liquid crystal layer is derived from the minimization of the free energy equation for the LC layer. The results of this are given by

$$\delta/\delta_0 = \frac{V_C}{V} \tanh \frac{V}{V_C} \qquad (1.5\text{-}1)$$

where V is the voltage across the cell, $\delta$ is the phase retardation, $V_C$ is a critical threshold voltage below which the liquid crystals remain stationary, and $\delta_0$ is the zero field phase retardation given by

$$\delta_0 = 2\pi \Delta n \, d/\lambda \qquad (1.5\text{-}2)$$

Here $\Delta n$ is the difference between the ordinary and extraordinary refractive indices of the liquid crystal, d is the thickness of the layer, and $\lambda$ is the incident light wavelength. The normalized retardation versus $V_C/V$ is shown in Fig. 1.5-3. For the case of perpendicular surface alignment, a closed form solution as given in Eq. (1.5-1) is not possible. However, numerical solutions to the minimized free energy equation yield the normalized phase retardation versus $V_C/V$ as shown in Fig. 1.5-4.

The CdS/CdTe photoconductor effectively switches the applied cell voltage $V_S$ onto the liquid crystal layer as a function of input light intensity. For input intensities much less than the saturation intensity of the photoconductor, the voltage appearing across the LC

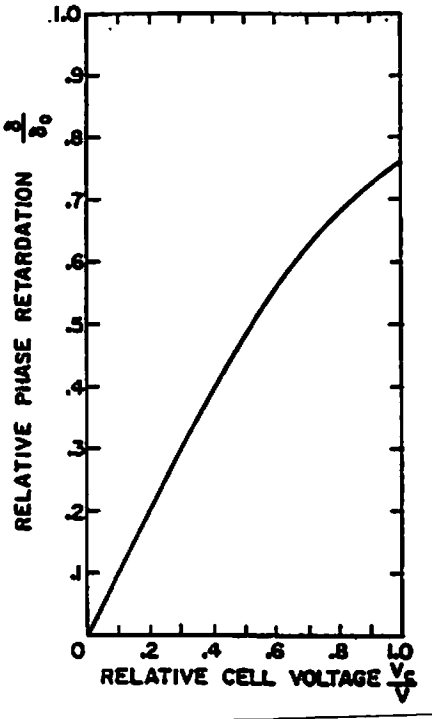


Figure 1.5-3 Phase vs. voltage$^{-1}$ for a parallel aligned cell.

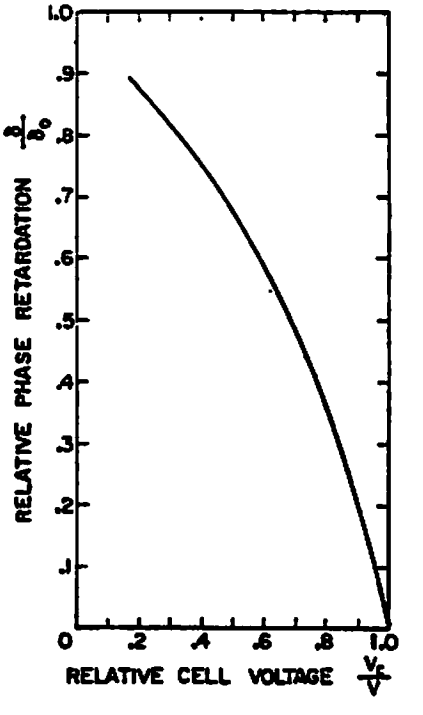


Figure 1.5-4 Phase vs. voltage$^{-1}$ for a perpendicular aligned cell.

layer is given by

$$V = C_1 V_S + C_2 \sqrt{I} \qquad (1.5\text{-}3)$$

where $C_1$ and $C_2$ are constants associated with the dark state impedance of the photoconductor, the impedances of the liquid crystal layer and dielectric films in the LCLV, and the conversion efficiency of the photoconductor.

As shown in Fig. 1.5-2, LCLV is used with the standard crossed polarizer ($P_1$)-analyzer($P_2$) readout configuration. Thus the light intensity emerging from $P_2$ toward lens $L_2$ is given by the relation

$$I = I_0 \sin^2\delta \qquad (1.5\text{-}4)$$

where $I_0$ is the incident read light intensity. Combining Eqs. (1.5-1) through (1.5-4) a theoretical plot of the device transfer function using typical device constants and a fixed bias voltage is shown in Fig. 1.5-5. The measured response of an actual LCLV is shown in Fig. 1.5-6. If the intensity is now held constant and the bias voltage is swept linearly over a specified voltage range, the log output intensity versus voltage (and therefore time) is shown in Fig. 1.5-7. The three responses shown in the figure are measurements for three different input intensities covering an input intensity range of 24 db. The finite null apparent in the data is a consequence both of the finite extinction ratio of the polarizer/analyzer pair used in the system and LCLV nonuniformities. Clearly each input intensity level in mapped into a unique null in time.

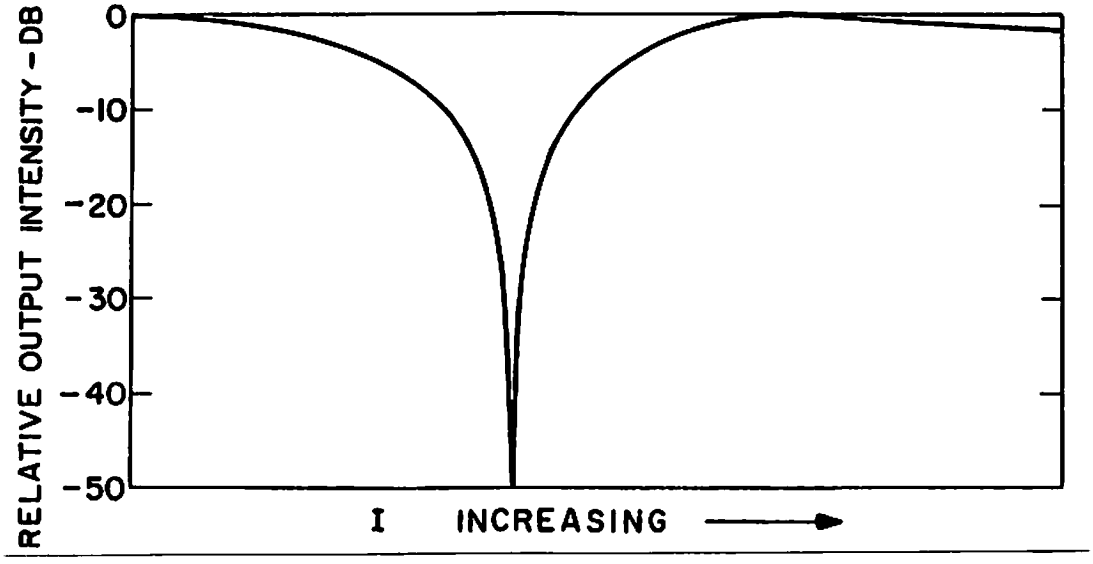


Figure 1.5-5 Theoretical intensity response for a parallel cell.

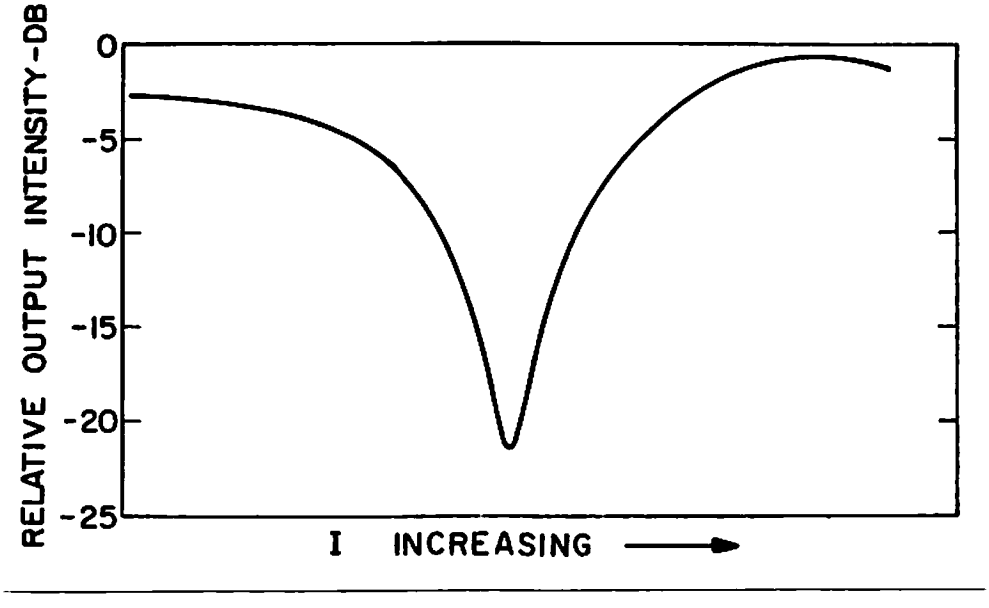


Figure 1.5-6 Measured intensity response for a parallel cell.

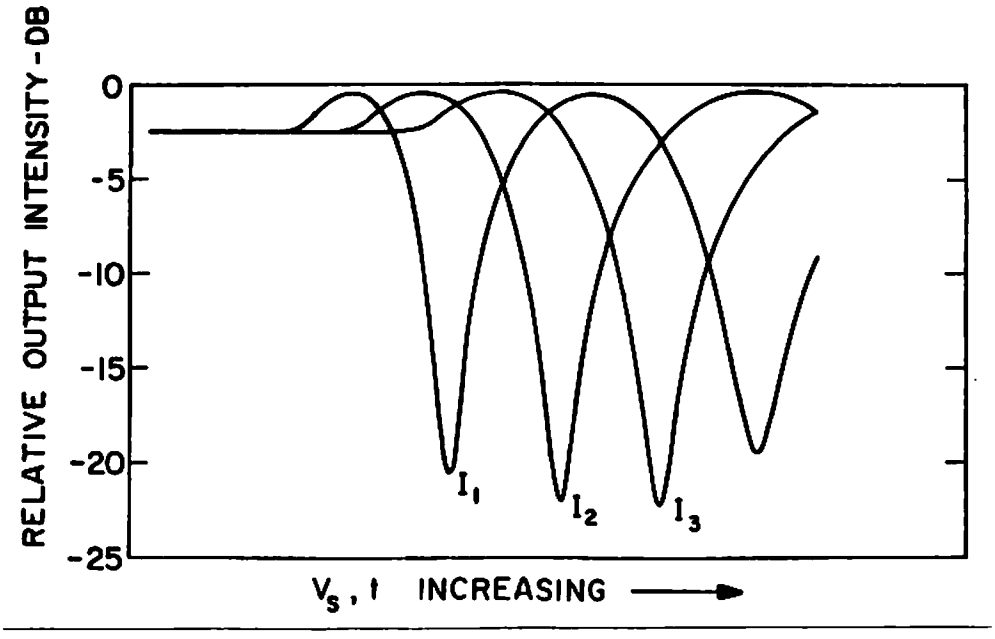


Figure 1.5-7 Measured voltage response for a parallel cell.

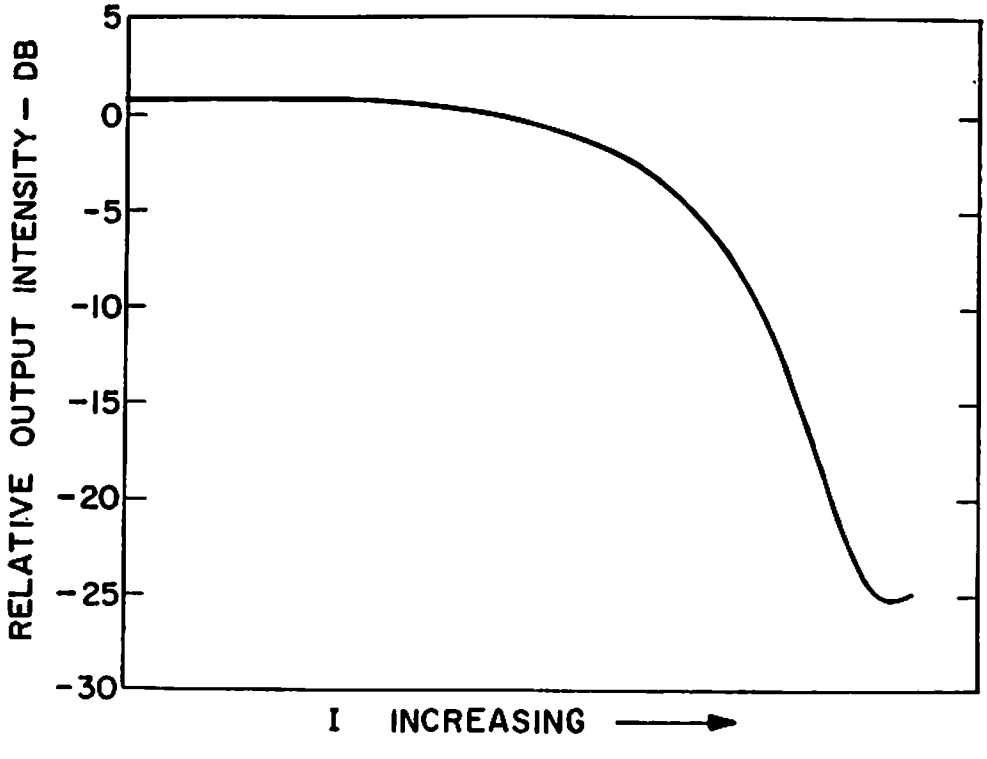


Figure 1.5-8 Transfer function for a twisted nematic cell.

Referring again to Fig. 1.5-2, $LCLV_2$ performs the dual role of reversing the contrast of the response from $LCLV_1$ and providing an intensity threshold. The device is of the twisted nematic type and together with the polarizer/analyzer pair, $P_3/P_4$, has the typical response shown in Fig. 1.5-8. Thus with proper threshold setting, accomplished by varying the read illumination $I_0$ to $LCLV_1$, the nulls shown in Fig. 1.5-7 become narrow intensity peaks in the plane to the right of $P_4$ in Fig. 1.5-2. The constant magnitude of the peaks is controlled by the level of the read illumination $I_1$ to $LCLV_2$.

$LCLV_3$ is a transmission type valve incorporating perpendicular liquid crystal surface alignment. Together with analyzer $P_5$, the device simply acts as an electrooptic attenuator whose transmission is set by the magnitude of the bias voltage $V_{S3}$. The bias voltage is controlled by a microprocessor which determines the proper time varied attenuation settings to achieve the desired system nonlinearity. The weighted intensity peaks emerging from $P_5$ are then collected over the two dimensional image space in the integrator depicted in Fig. 1.5-2. Although shown as a vidicon in the figure, experimentally the integration was performed on photographic film. Figure 1.5-9b shows the experimental results of a level slice operation being performed on the variable intensity input image of Fig. 1.5-9a.

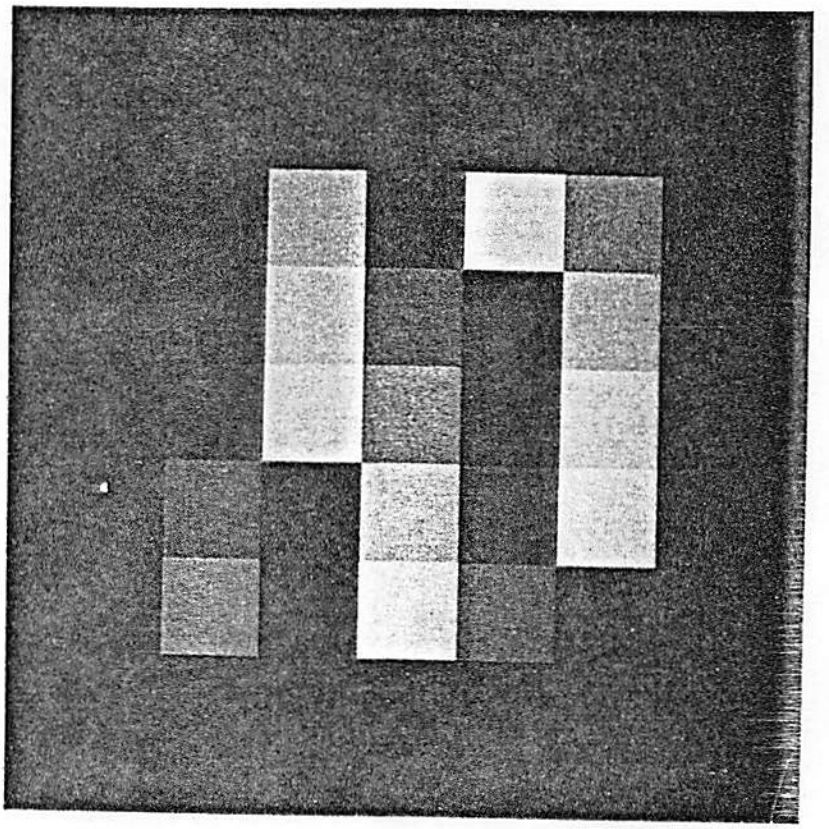

(a)

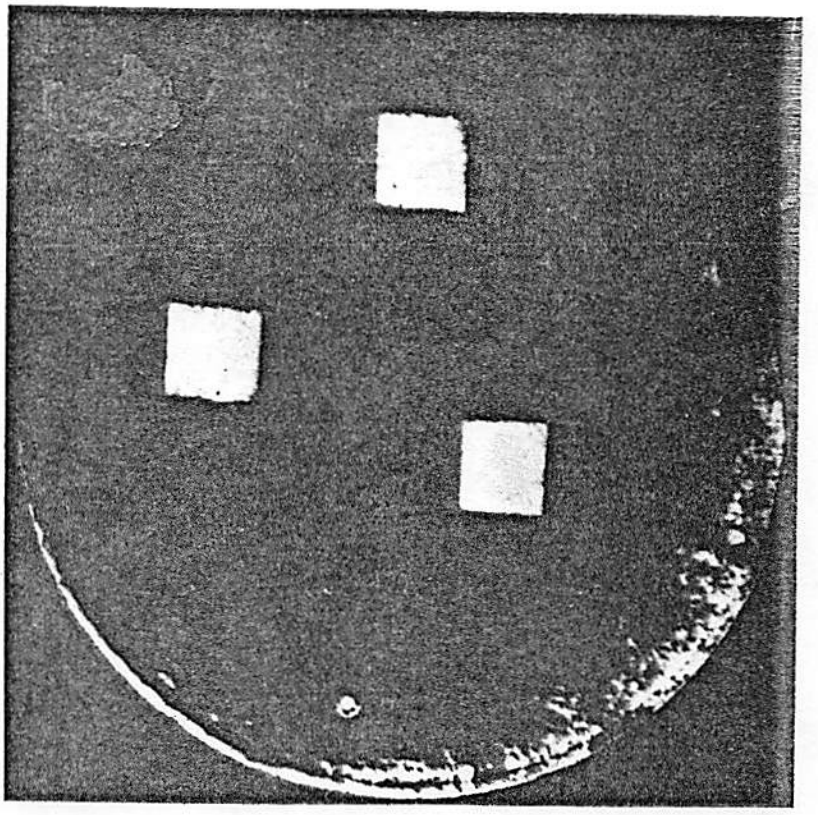

(b)

Figure 1.5-9 Level slice operation:a) Input image. b) Processed image.

## 1.6 Variable Grating Mode Processing with Intensity-to-Spatial Frequency Conversion

One of the major consequences of this cooperative effort between USC and the Hughes Research Laboratories (HRL) has been the identification of the variable grating mode (VGM) effect in liquid crystals as a potentially powerful new tool in optical processing [15-17,19,27,28]. Although the VGM effect is known to most people doing research in liquid crystal devices, it has received relatively little attention since it is not useful in normal display applications. However, as we have found, such a device could have very important applications in optical processing, in particular for the direct implementation of arbitrary nonlinear functions in real time. Using this approach, it should be possible to implement an arbitrary nonlinearity without the use of halftone techniques. The extent to which this can be used depends upon the exact character of the VGM effect which is being studied by HRL.

The idea behind utilizing the VGM effect for nonlinear processing is quite simple. Under certain conditions a linear, phase grating structure can be established in a liquid crystal (LC). The period of this grating can be varied by changing the externally applied voltage across the LC. By adding a photoconductive electrode to the LC cell, the effective voltage, and thus the grating frequency, should follow the intensity variations of an image projected onto the photoconductor. Thus the device would act like an intensity-to-spatial frequency converter capable of operating on

two-dimensional images. If this VGM encoded image were the input to an optical spatial filtering system, the different spatial frequency components would appear at different locations in the frequency plane and could be filtered to produce an output with any desired nonlinear relationship to the input frequency, and thus to the original input intensity.

Gray Level Resolution of a VGM Device

A detailed theoretical analysis of this variable grating mode approach to nonlinear processing is given in a companion report, USCIPI Report 880 [20]. For purposes of this report it is important to consider the question of gray level resolution or dynamic range limitations inherent in the VGM technique.

In order to have a unique mapping of intensity to spatial frequency, one must restrict the range of input intensities. Figure 1.6-1 depicts an idealized response curve for a VGM device. In general the grating consists of not only some fundamental component, but also higher harmonic components. The first significant harmonic will generally occur at twice the fundamental frequency. However, experimental observations show that this order can in some instances be eliminated, in which case the first significant harmonic occurs at three times the fundamental. The VGM device can only be operated unambiguously in the frequency range between the lowest fundamental frequency and its first significant harmonic. This is shown as the cross-hatched area in Fig. 1.6-1. This usable frequency range will be referred to as $\Delta\nu$.

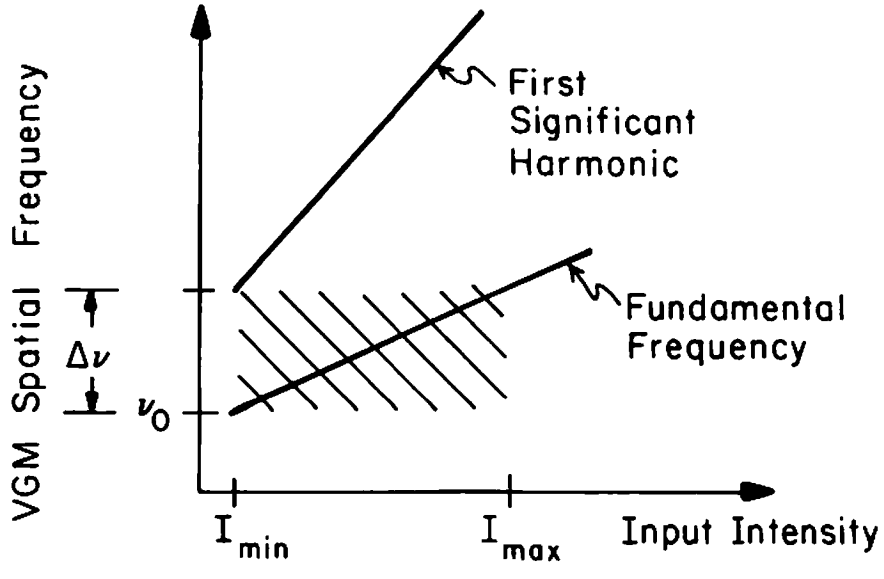


Figure 1.6-1 Region of unique intensity-to-spatial frequency mapping.

Due to the finite width of the object spectrum the number of uniquely addressable spatial frequencies in the range $\Delta\nu$ is limited. (See Fig. 1.6-2). The number of uniquely addressable spatial frequencies is in turn equivalent to the number of independent gray levels that can be processed. The extent of the object spectrum can be approximated as 2/b where b is the size of the smallest resolution element (pixel) in the image. Thus if we wish to distinguish N intensity levels, the pixel size and the spatial frequency operating range must satisfy the condition

$$2/b \leq \Delta\nu/N \tag{1.6-1}$$

or

$$b \geq 2N/\Delta\nu \tag{1.6-2}$$

Although as noted earlier it may be possible to eliminate the first harmonic component of the VGM spectrum, for purposes of "worst case" analysis we will assume that it is present. In this case, if the lowest VGM frequency component is $\nu_0$, then the usable frequency range $\Delta\nu$ is

$$\Delta\nu = 2\nu_0 - \nu_0 = \nu_0 \tag{1.6-3}$$

Substituting this into the previous equation and rewriting gives the result

$$b \geq 2N/\nu_0 \tag{1.6-4}$$

This says that the pixel size must be such that it spans 2N periods of

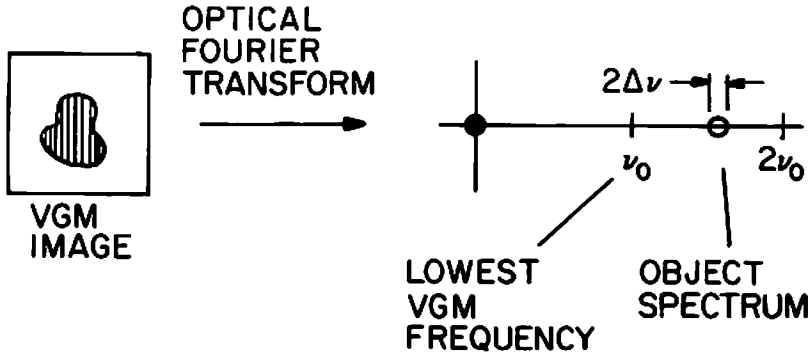


Figure 1.6-2 Gray level resolution with VGM. The number of resolvable gray levels depends upon the ratio of the object spectrum extent to the separation of the grating harmonics.

the lowest grating frequence if we want to process N gray levels.

As an example, if $\nu_0$= 200 cycles/mm and N = 50, then each pixel must have a size b = 0.5 mm. Thus if the device has a 50 mm square aperture, then a 100 x 100 pixel image could be processed.

Experimental Results with VGM Devices

The experimental work in the past year in the area of VGM devices has been concentrated on producing a device with a good lifetime and one which produces well-defined diffraction orders when placed in an optical Fourier transform system. One device has also been used for a preliminary demonstration of the VGM technique. The demonstration experiment consisted of realizing an electrically controllable level slice. The level slice operation is performed by projecting an image on the VGM device and spatial filtering the resulting image with a simple slit placed in the Fourier plane. The VGM device performs an intensity-to-spatial frequency transformation on the input. The slit then transmits only a selected range of spatial frequencies. Only the portions of the input image whose intensities correspond to the selected spatial frequencies are seen in the final image. Thus a level slice is effected. The level slice window can be moved by varying the bias voltage on the VGM device. All of this experimental work with the VGM devices has been conducted at HRL. A detailed account of this work can be found in the HRL 1979 Annual Technical Report for contract number F49620-77-C-0080.

As discussed earlier, higher order harmonic components are

deterimental to the theoretically realizable gray level dynamic range and gray level resolution of the VGM cell. Recently, a joint USC-Hughes experimental program has been initiated to determine the fundamental nature of the phase grating profile. The Fourier transform of the profile yields the relative magnitudes of the higher order harmonic components. Initial experiments showed that alternating diffracted orders (up to eigth order) are orthogonally polarized. This observation allows for a doubling of the gray scale dynamic range by simple output polarization state selection techniques. Experiments to measure the relative magnitudes of the diffracted orders (to fit to theoretical models of the phase profile), and to attempt direct imaging of the phase profile under high magnification in a polarization microscope (which involves development of a VGM cell with a very thin upper glass plate to allow for concomitant small focal working distances) are in progress.

## Advantages of Nonlinear Processing with a VGM Device

There are several advantages to this system over the halftone process. The most obvious is that it does not require a halftone screen. The production of a screen with a large bandwidth and the extremely accurate gray-scale resolution necessary for halftone processing is a major difficulty associated with the halftone approach. With the VGM approach, it is also very easy to change the nonlinearity to be implemented. With the halftone technique, one generally needs a different halftone screen for each nonlinearity and perhaps a different filter also. With the VGM approach, one simply

changes the filter. The filters inherently require only modest resolution as opposed to the halftone screens.

## 1.7 Alternative Devices for Nonlinear Optical Processing

A wide range of spatial light modulator characteristics are necessary for successful implementation of nonlinear optical processing algorithms in real time. In order to complement the liquid crystal device research at Hughes (and, primarily in the case of the variable grating mode cell, at USC), several promising alternative device technologies are under investigation. Of the numerous distinct classes of nonlinear device characteristics being examined, those with the highest priority are devices with sharp threshold responses for real-time processing with accompanying halftone techniques and for implementation of the multiple light valve intensity-to-temporal nonlinear modulation scheme. In addition, characteristics of Pockels Readout Optical Modulators (PROM's) are being investigated for possible use as the input spatial light modulator, thresholding and inverting device, and output plane temporal integrator for the multiple light valve system. Progress in each of these principal areas of investigation is outlined below.

### Devices with Sharp Threshold Characteristics

Several concepts aimed at attaining sharp threshold transfer functions have been explored during the past year, including modulated frustrated total internal reflection, optical feedback, use of ferroelectric domain bistability in ambidextrous crystals, and appropriate modification of PROM image transfer characteristics.

The total internal reflection (TIR) approach involves image-wise

modulation of the index of refraction at the interface between two dissimilar optical materials, altering the critical angle for total internal reflection. A theoretical model of such a device (shown schematically in Fig. 1.7-1) was constructed, and the reflected beam intensity was numerically evaluated by solution of the Fresnel equations. A careful analysis of this configuration revealed that for a p-polarized (parallel to the plane of incidence) readout beam, the Brewster angle (at which the reflected intensity vanishes) can be made arbitrarily close to the critical angle (at which the reflected intensity reaches 100% of the incident intensity) for increasing values of the ratio $n_1/n_2$ of the indices of refraction in the two materials. This situation is illustrated schematically in Fig. 1.7-2, where it can be easily seen that the sharpness (effective $\gamma$) of the threshold increases with increasing $n_1/n_2$. However, even for values of $n_1/n_2$ of order 5 (reasonably difficult to achieve in a physical system), the electric field strength required to modulate the critical angle over an appropriate range approaches the dielectric breakdown strength of most optical materials (about $1 \times 10^6$ V/cm). The separation between the critical angle and the Brewster angle is given simply by

$$\Delta\Theta = \Theta_C - \Theta_B = \sin^{-1}\left[\frac{n_2}{n_1}\right] - \tan^{-1}\left[\frac{n_2}{n_1}\right] \qquad (1.7\text{-}1)$$

with $n_1 > n_2$ the relevant indices of refraction in the two materials. From the results of the above study, it was concluded that low contrast (25:1) thresholding is possible using TIR devices with

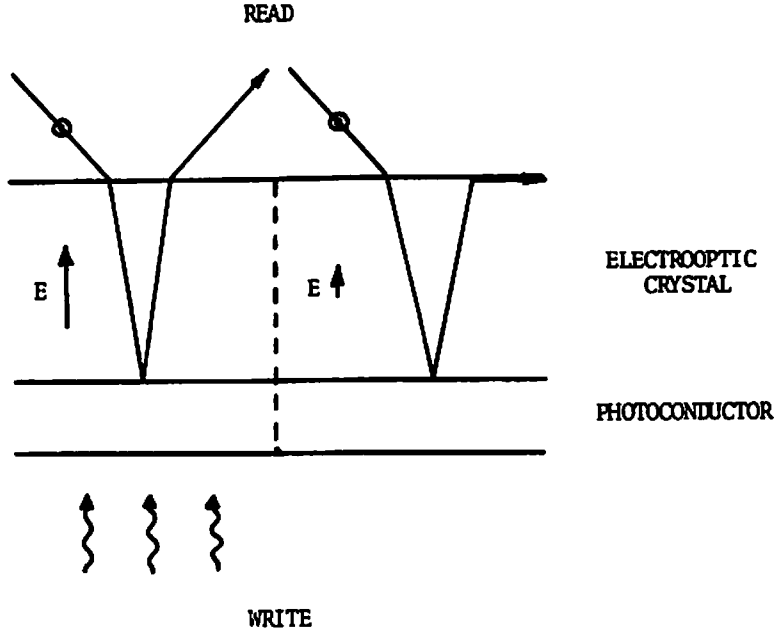


Figure 1.7-1 Schematic diagram of a possible image thresholding device showing operation by modulated total internal reflection.

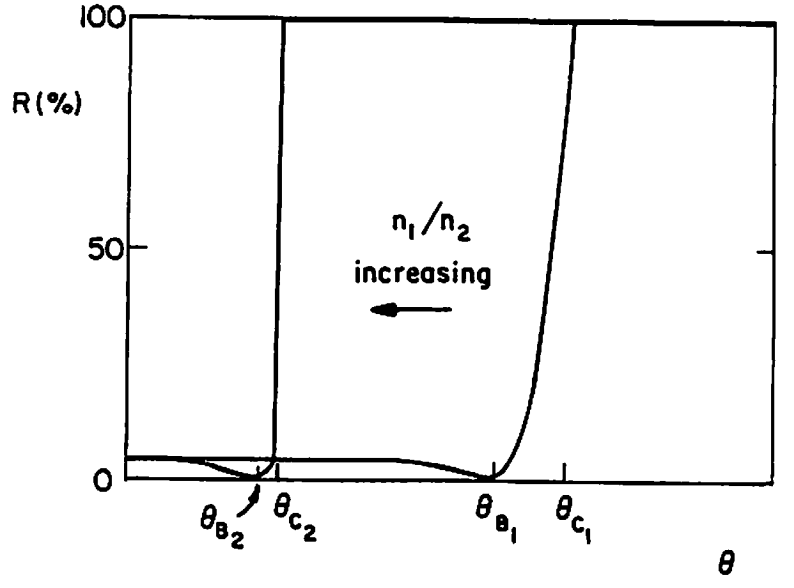


Figure 1.7-2 Plot of the reflection coefficient (R) as a function of the incidence angle ($\theta$) for two separate values of the ratio of indices of refraction $n_1/n_2$.

presently available materials, but that high contrast (100:1) thresholding awaits development of optical materials with much larger electrooptic coefficients than those presently available.

The use of optical feedback in conjunction with the Hughes Liquid Crystal Light Valve (LCLV) has been discussed previously [42,47]. Here the intrinsic gain available in the positive feedback loop was found to increase significantly the slope of the output intensity vs. input intensity characteristic curve, although at a cost in response time of the system. Several schemes for extending such feedback techniques to the PROM electrooptic spatial light modulator were generated during the present grant period. Evaluation of these feedback techniques for possible use in image thresholding is in progress.

A third approach to the development of a spatial light modulator with a sharp threshold characteristic involves the utilization of bistable ferroelectric domains in ambidextrous crystals (see Fig. 1.7-3). Ambidextrous crystals may exhibit either handedness of optical activity (dextrorotatory or laevorotatory) depending on the poling history of a given ferroelectric domain in the material. The domains may be easily switched from one handedness to the other by appropriate application of a voltage pulse. Since the switching time for a given domain is found to be a strongly nonlinear function of the magnitude of the voltage pulse [29], it is conceivable that application of an image-wise modulated voltage pulse for a given duration will switch only those domains for which the voltage is above

AMBIDEXTROUS CRYSTALS (BISTABLE OPTICAL ACTIVITY)

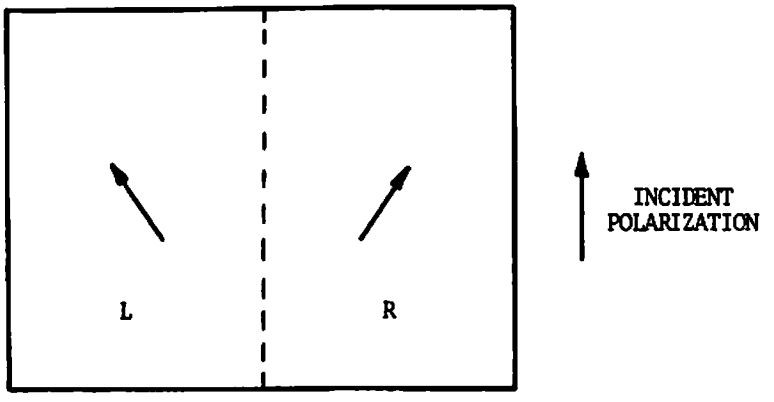


$Pb_5Ge_3O_{11}$

Figure 1.7-3 Schematic diagram of two adjacent domains of opposite handed optical activity in the ambidextrous crystal lead germanate ($Pb_5Ge_3O_{11}$). Such crystals are possible candidates for bistable (two state) spatial light modulators. The arrows represent the polarization direction of light emerging from each domain relative to the incident polarization shown.

threshold. Since the output state of the device is intrinsically bistable, variable thresholding could thus be implemented by merely varying either the applied bias or the pulse duration. A photoconductor-ferroelectric sandwich device was fabricated by Cummins and Luke [30], and demonstrated excellent constrast (>200:1) and resolution (>100 lp/mm). However, no data was given on the optical transfer function relating output intensity to input (writing) intensity, and the device was not exposed to grey scale images. During the present grant period, a single crystal sample of $Pb_5Ge_3O_{11}$ has been obtained from Philips Research Laboratory in order to investigate the pulse magnitude/duration switching characteristics. An experimental apparatus is in process of being assembled to measure the statistical distribution of switching times for domains poled by variable magnitude, variable duration voltage pulses. Continuation of work on this particular project was postponed to await the development of thin film sputtering capability anticipated during the summer, 1979; such capability will allow depositions of appropriate transparent conductive contacts (field plates) and photoconductive thin films necessary for the proper evaluation of the potential of this proposed thresholding device.

Several possible modifications of the Pockels Readout Optical Modulator (PROM) operational sequence have been derived for ongoing evaluation. One possible modification involves exposure of the PROM to write light at a wavelength coresponding to a very large optical absorption coefficient, so that all electron-hole pairs are created within a few microns of one BSO-insulator interface. In this case,

electrons migrate on the average one drift length (10-15 microns) before being trapped, leading to a strongly non-monotonic reduction in the electrostatic potential. The resultant exposure curve [31] shows a sharp rise and a distinct saturation region that may be usable as a thresholding function. A second possible modification involves selective erasure of regions in the PROM exposed below a cetain threshold by adjusting the external bias during the write cycle (a form of voltage modulated recording). Finally, an analysis has been performed that predicts substantial improvement in the effective $\gamma$ of the PROM transfer function for sequential exposure onto succeeding PROMs - essentially a sequential multiple pass optical feedback configuration. Since in the normal PROM operating mode the output intensity is a quadratic function of the input intensity, sequential re-exposure from PROM to PROM should increase the effective $\Upsilon$ by a factor of 2 for every stage, achieving a $\gamma$ of 8 for only two subsequent exposures. During the grant period, a PROM device and flexible support electronics were obtained from Itek Corporation (Lexington, Massachusetts) to allow these modifications to be investigated on both commercially available devices and those fabricated at USC (the USC fabrication facility will be fully operational with the addition of an rf magnetron sputtering system, as described more fully in the renewal proposal for 1979-1980). A vibration isolated optical table has been purchased and installed for dedicated real-time device evaluation, and appropriate PROM optics and support electronics have been assembled and tested prior to initiation of the device evaluation and modification effort.

PROM Evaluation and Improvement

As noted in the discussion concerning the multiple light valve intensity-to-temporal nonlinear modulation scheme (Section 1.5), several distinct types of real-time spatial modulators will be required for optimum system implementation and performance evaluation. Spatial light modulators must be developed that will perform (1) input incoherent-to-coherent conversion with reasonable image linearity, (2) image thresholding and inversion, and (3) output plane temporal integration over the scanning grey scale cycle time. We are presently actively engaged in evaluation of the PROM as a potential candidate for these functions. The PROM is seemingly ideal for the input and output functions, and is a possible candidate for the thresholding and inversion function as described above. Progress to date consists primarily in assembly and test of the PROM evaluation facilities, and in a promising theoretical and experimental investigation of the resolution-limiting factors in PROM design and operation funded by the Joint Services Electronics Program and the National Science Foundation, but strongly impacting the alternative nonlinear device effort. This investigation has already yielded a number of interesting and significant results. The theoretical approach to the resolution problem initially involved deriving the electrostatic field distribution from a fixed distribution of point charges located at the interface between two dissimilar dielectrics bounded by ground planes. The electric field modulation resulting from a periodic array of charges of given spatial frequency can be directly related to the

exposure dependent modulation transfer function of the device. We have obtained an analytic expression for the Fourier transform of the voltage distribution from a single point charge (which is also directly related to the modulation transfer function) for the full three layer dielectric problem, and have extended the theory to include the dependence of the voltage distribution on the point charge location within the electrooptic crystal. The resultant analytic expression contains the dielectric constants of the blocking layers and electrooptic crystal, and the thicknesses of the three layers, as well as the location of the point charge. This formulation allows the effects of charge trapping within the bulk of the electrooptic crystal to be modeled. In particular, the low spatial frequency response decreases linearly, and the high spatial frequency response decreases exponentially with the distance of the point charge from the electrooptic crystal/dielectric blocking layer interface. Thus the overall sensitivity and resolution are degraded strongly by charge storage in the bulk away from the interface. Utilizing superposition, this formulation can be readily extended to accommodate arbitrary charge distributions of particular physical interest.

These results have numerous implications with regard to improving the current resolution limitations of the PROM. In particular, the results indicate that substantial gains in PROM resolution are achievable, provided that the parylene blocking layer be replaced with a high dielectric constant, high dielectric breakdown strength insulating layer with appropriate optical quality. A typical example of such resolution enhancement is shown in Figs. 1.7-4 and 1.7-5.

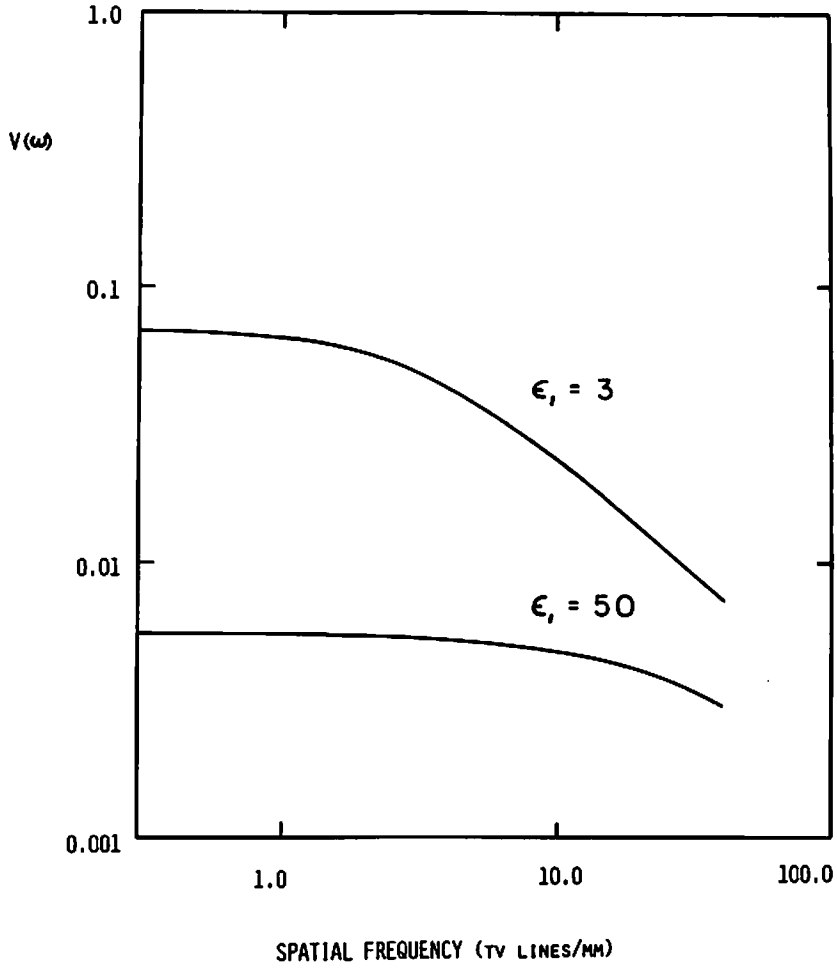


Figure 1.7-4 Plot of the Fourier transform of the electrostatic potential in a PROM structure (related to the modulation transfer function) as a function of spatial frequency with the dielectric constant of the blocking layer as a parameter.

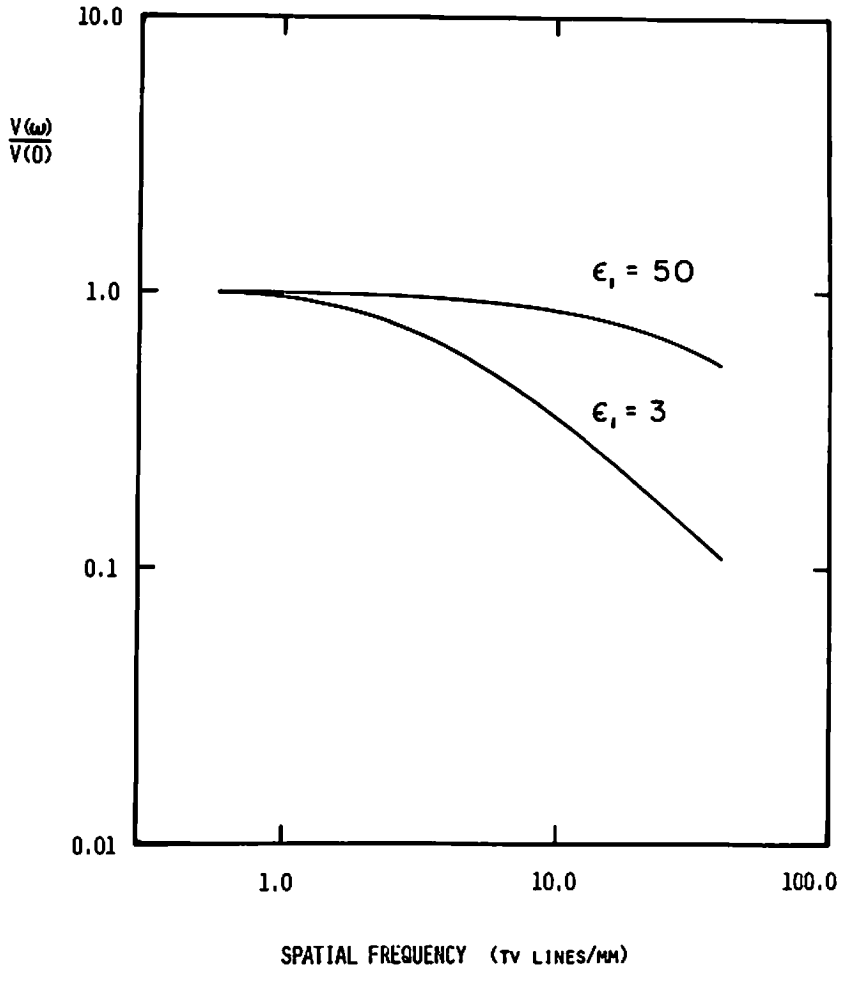


Figure 1.7-5 Normalized plot of the Fourier transform of the electrostatic potential in a PROM structure (related to the modulation transfer function) as a function of spatial frequency with the dielectric constant of the blocking layer as a parameter.

Figure 1.7-4 shows a plot of the Fourier transform of the electrostatic potential in a PROM structure (related to the modulation transfer function) with the dielectric constant of the blocking layer as a parameter, for equal exposure in both cases. The curve with $\varepsilon = 3$ is representative of performance expected with parylene blocking layer devices, whereas the curve with $\varepsilon = 50$ shows the increase in high spatial frequency cutoff predicted for blocking layer materials similar to bismuth silicon oxide ( $\varepsilon = 56$). A normalized plot is shown in Fig. 1.7-5, representing the same two devices as in the previous figure, with writing exposure chosen to equate the two curves at low spatial frequencies. The spatial frequency response enhancement in the case of the higher dielectric constant blocking layer is striking. High quality insulating thin films characterized by appropriately large dielectric constants are not presently available. However, the relatively new thin film deposition technique of rf magnetron sputtering shows great promise for the development of single and multilayer dielectric coatings with the requisite characteristics and quality. Continuation of this line of investigation is contingent on installation of an rf magnetron sputtering system for optical thin film deposition.

Alternative Nonlinear Device Fabrication

The capability of flexible test structure and device fabrication is exceedingly important to the success of the alternative nonlinear device effort. Such capability encompasses a wide range of technologies, almost all of which were fully developed and tested

during the grant period. Single crystal boule orientation, crystal cutting, optical polishing, and electron beam deposition of thin metallic transparent conductive coatings have been accomplished. A Sloan electron beam gun evaporator has been modified to accommodate a new substrate support system with an integral quartz crystal digital thickness monitor for accurate conrol of optical quality thin film deposition. A parylene coating unit for fabrication of PROM test structures has been assembled for preliminary parylene deposition runs. Characterization measurements will include tests of dielectric breakdown strength, thickness uniformity, and optical transmission as a function of wavelength (to determine transparency in the visible spectrum as well as the amount of un-polymerized dimer in the resultant films).

An existing Czochralski crystal pulling apparatus is being overhauled and modified for growth and doping experiments with bismuth silicon oxide and other optical materials. The growth furnace consists of two independently controlled zones for adjustment of the furnace thermal profile and post-growth annealing. Detailed thermal profiling (measurement and furnace optimization) is nearing completion. Commencement of pulling experiments now awaits delivery of a back-ordered pair of solid state power controllers.

A high temperature annealing furnace with associated ultrapure gas flow equipment has been assembled and characterized for use in thermal annealing of as-grown boules and as-cut wafers to reduce residual birefringent strain. Annealing capability exists for thermal

treatments in ultrapure oxygen, ultrapure nitrogen and ultrapure forming gas (3% $H_2$ in $N_2$) from room temperature to 1200$^{o}$C.

The only remaining technology requisite for completion of fully capable device fabrication facilities is that of rf magnetron sputtering. In the final months of the grant year, emphasis was placed primarily on necessary preparations in anticipation of the acquisition of the rf magnetron sputtering system. A cryogenic fore-pumped, oil-free ion pumped vacuum station was obtained, and has undergone extensive and continuing characterization and modification to allow optimum mating to the Sloan 18" sputtering configuration, to assure rapid cycle times, and to maintain the high constant differential pressure of inert gases requisite for low contamination, high optical quality and dielectric integrity sputtered thin films. The completed sputtering system is a major asset to the device program, providing capability for high transparency high conductivity coatings (such as indium tin oxide and cadmium tin oxide) for use as field plates and longitudinal device contacts, novel thin insulating films of excellent dielectric and optical properties, and (eventually) high performance photoconductors in thin film form.

## 1.8 References


1. Special Issue on Optical Computing, Proc. IEEE, Vol. 65, January 1977.

2. H.C. Andrews, A.G. Tescher, and R.P. Kruger, "Image Processing by Digital Computer," IEEE Spectrum, Vol. 9, No. 7, pp. 20-32, 1972.

3. J.W. Goodman, Introduction to Fourier Optics, McGraw-Hill, New York, 1968.

4. J.W. Goodman, "Operations Acchievable With Coherent Optical Information Processing Systems," Proc. IEEE, Vol 65, pp. 29-38, 1977.

5. B.J. Thompson, "Hybrid Processing Systems - An Assessment," Proc. IEEE, Vol. 65, pp. 62-76, 1977.

6. H. Kato and J.W. Goodman, "Nonlinear Filtering in Coherent Optical Systems Through Halftone Screen Processes," Applied Optics, Vol. 14, pp. 1813-1824, 1975.

7. T.C. Strand, "Non-monotonic Nonlinear Image Processing Using Halftone Techniques," Optics Communications, Vol. 15, pp. 60-65, 1975.

8. S.R. Dashiell and A.A. Sawchuk, "Optical Synthesis of Nonlinear Nonmonotonic Functions," Optics Communications, Vol. 15, pp. 66-70, 1975.

9. S.R. Dashiell and A.A. Sawchuk, "Nonlinear Optical Processing: Analysis and Synthesis," Applied Optics, Vol. 16, pp. 1009-1025, 1977.

10. S.R. Dashiell and A.A. Sawchuk, "Nonlinear Optical Processing: Nonmonotonic Halftone Cells and Phase Halftones," Applied Optics, Vol. 16, pp. 1936-1943, 1977.

11. S.R. Dashiell and A.A. Sawchuk, "Nonlinear Optical Processing: Effects of Input Medium and Precompensation," Applied Optics, Vol. 16, pp. 2279-2287, 1977.

12. H.K. Liu, J.W. Goodman, and J. Chan, "Equidensitometry by Coherent Optical Filtering," Applied Optics, Vol. 15, pp. 2394-2399, 1976.

13. H.K. Liu and J.W. Goodman, "A New Coherent Optical Pseudo-Color Encoder," Nouv. Rev. Optique, Vol. 7, pp. 285-289, 1976.

14. H.K. Liu, "Coherent Optical Analog-to-Digital Conversion Using a Single Halftone Photograph," Applied Optics, Vol. 17, pp. 2181-2185, 1978.

15. A.A. Sawchuk, et al., "Nonlinear Real-Time Optical Signal Processing," Report 820, USC Image Processing Institute, Los Angeles, Ca. 90007, June 15, 1978.

16. A. Armand, D. Boswell, A.A. Sawchuk, B.H. Soffer and T.C. Strand, "Real-Time Nonlinear Optical Processing with Liquid Crystal Devices," Proceedings IEEE 1978 International Optical Computing Conference, London, pp. 153-158 (September 1978).

17. A. Armand, D. Boswell, A.A. Sawchuk, B.H. Soffer and T.C. Strand, "Approaches to Nonlinear Optical Processing in Real Time," Proceedings International Commission For Optics Congress, Madrid, Spain, pp. 253-256, (September 1978).

18. A. Armand, D. Boswell, J. Michaelson, A.A. Sawchuk, B.H. Soffer, and T.C. Strand, "Real-Time Nonlinear Processing with Halftone Screens," 1978 Annual Meeting, Optical Society of America, San Francisco, October 1978, Journal Optical Society of America, Vol. 68, pp. 1361, (October 1978).

19. A. Armand, D. Boswell, A.A. Sawchuk, B.H. Soffer, and T.C. Strand, "New Methods for Real-Time Nonlinear Optical Processing," 1978 Annual Meeting, Optical Society of America, San Francisco, October 1978, Journal Optical Society of America, Vol. 68, pp. 1361, (October 1978).

20. A. Armand, "Real-Time Nonlinear Optical Information Processing," Report 880, USC Image Processing Institute, Los Angeles, Ca. 90007, June 1979.

21. A.V. Oppenheim, R.W. Schaefer, and T.G. Stockham, Jr., "Nonlinear Filtering of Multiplied and Convolved Signals," Proc. IEEE, Vol. 56, pp. 1264-1291, 1968.

22. D. Casasent, "A Hybrid Image Processor," Optical Engineering, Vol. 13, pp. 228-234, 1974.

23. S. Iwasa and J. Feinleib, "The PROM Device in Optical Processing

Systems," Optical Engineering, Vol. 13, pp. 235-242, 1974.

24. D. Casasent, "Spatial Light Modulators," Proc. IEEE, Vol. 65, pp. 143-157, 1977.

25. T.D. Beard, W.P. Bleha, S-Y. Wong, "AC Liquid/Crystal light Valve," Appl. Phys. Lett., Vol. 22, pp. 90-92, 1974.

26. J. Grinberg, et al., "A New Real-Time Non-Coherent to Coherent Light Image Converter," Optical Engineering, Vol. 14, pp. 217-225, 1975.

27. J.M. Pollack and J.B. Flannery, "A Low-Noise Image Amplifier," Society for Information Display 1976 International Symposium Digest, pp. 142-145, 1976.

28. J.D. Margerum and L.J. Miller, "Electro-Optical Applications of Liquid Crystals," J. of Colloid and Interface Science, (1977); Hughes Research Laboratories Research Report 499, June 1976.

29. H. Iwasaki, K. Sugii, N. Niizeki and H. Toyoda, "Switcing of Optical Rotatory Power in Ferroelectric $5PbO.3GeO_2$ Single Crystal," Ferroelectrics, Vol. 3, pp. 157-161, 1972.

30. S.E. Cummins and T.E. Luke, "Image Storage in a Ferroelectric-Photoconductor Device Structure Using Single-Crystal $Pb_5Ge_3O_{11}$," Proc. IEEE, pp. 1039-1040, 1973.

31. R.A. Sprague, "Effect of Bulk Carriers on PROM Sensitivity," J. Appl. Phys., Vol. 46, pp. 1673-1678, 1975.

## 2. PROFESSIONAL PERSONNEL

The following individuals contributed to the research effort supported by this grant:

1. Alexander A. Sawchuk, Associate Professor, Department of Electrical Engineering, Director - Image Processing Institute, Principal Investigator.
2. Timothy C. Strand, Research Assistant Professor, Image Processing Institute, Senior Investigator.
3. Armand R. Tanguay, Jr., Assistant Professor, Departments of Electrical Engineering and Materials Science, and Image Processing Institute, Senior Investigator.
4. Ahmad Armand, Research Assistant, Ph.D. Graduate, Department of Electrical Engineering.
5. Jerry D. Michaelson, Research Assistant, Ph.D. Candidate, Department of Electrical Engineering.
6. Gerard Ashton, Senior, Department of Electrical Engineering.
7. Michael Muha, Senior, Department of Physics.

The following individuals have received degrees from the University of Southern California while participating in the research effort:

1. Ahmad Armand, Ph.D., Electrical Engineering, June 1979, thesis title: "Real-Time Nonlinear Optical Information Processing."
2. Gerard Ashton, B.S., Electrical Engineering, June 1978.
3. Michael Muha, B.S., Physics, June 1979.

## 3. PUBLICATIONS

This section lists written publications resulting from AFOSR support from the initial starting date.


1. S.R. Dashiell and A.A. Sawchuk, "Nonlinear Optical Processing: Analysis and Synthesis," Applied Optics, Vol. 16, pp. 1009-1025, (April 1977).

2. S.R. Dashiell and A.A. Sawchuk, "Nonlinear Optical Processing: Non-monotonic Halftone Cells and Phase Halftones," Applied Optics, Vol. 16, pp. 1936-1943, (July 1977).

3. S.R. Dashiell and A.A. Sawchuk, "Nonlinear Optical Processing: Effects of Input Medium and Precompensation," Applied Optics, Vol. 16, pp. 2279-2287, (August 1977).

4. A. Armand, D. Boswell, A.A. Sawchuk, B.H. Soffer and T.C. Strand, "Real-Time Nonlinear Optical Processing with Liquid Crystal Devices," Proceedings 1978 International Optical Computing Conference, London, pp. 153-158, (September 1978).

5. A. Armand, D. Boswell, A.A. Sawchuk, B.H. Soffer and T.C. Strand, "Approaches to Nonlinear Optical Processing in Real-Time," Proceedings International Commission for Optics Congress, Madrid, Spain, pp. 253-256, (September 1978).

6. A.A. Sawchuk and T.C. Strand, "Nonlinear Image Processing," in Applications of Optical Fourier Transforms, H. Stark, to appear ed., Academic, New York, (1979).

7. A. Armand, D. Boswell, J. Michaelson, A.A. Sawchuk, B.H. Soffer and T.C. Strand, "Real-Time Nonlinear Processing with Halftone Screens," 1978 Annual Meeting, Optical Society of America, San Francisco, October 1978, Journal Optical Society of America, Vol. 68, p. 1361, (October 1978).

8. A. Armand, D. Boswell, A.A. Sawchuk, B.H. Soffer and T.C. Strand, "New Methods for Real-time Nonlinear Optical Processing," 1978 Annual Meeting, Optical Society of America, San Francisco, October 1978, Journal Optical Society of America, Vol. 68, p. 1361, (October 1978).

9. J. Michaelson, "Liquid Crystal Threshold and Gamma Improvement Using Optical Feedback," submitted for publication to Optics Letters.

## 4. ORAL PRESENTATIONS

This section lists oral presentations at meetings and conferences describing research supported by this grant.

1. A. Armand, D. Boswell, A.A. Sawchuk, B.H. Soffer and T.C. Strand, "Approaches to Nonlinear Optical Processing with Liquid Crystal Devices," presented at the 1978 International Optical Computing Conference, London, (September 1978).

2. A. Armand, D. Boswell, A.A. Sawchuk, B.H. Soffer and T.C. Strand, "Approaches to Nonlinear Optical Processing in Real-Time," presented at the International Commission for Optics Congress, Madrid, Spain, (September 1978).

3. A. Armand, D. Boswell, J. Michaelson, A.A. Sawchuk, B.H. Soffer and T.C. Strand, "Real-Time Nonlinear Processing with Halftone Screens," presented at 1978 Annual Meeting, Optical Society of America, San Francisco, (October 1978).

4. A. Armand, D. Boswell, A.A. Sawchuk, B.H. Soffer and T.C. Strand, "New Methods for Real-Time Nonlinear Processing," presented at 1978 Annual Meeting, Optical Society of America, San Francisco, (October 1978).